Journal of Ayurveda and Integrative Medicine 16 (2025) 101085

Contents lists available at ScienceDirect

Journal of Ayurveda and Integrative Medicine

journal homepage: elsevier.com/locate/jaim

Review Article

Plants used in *Ayurveda* for *Jwara* or fever: A review of their antiviral studies

Athira Bindhu, Ajikumaran Nair S, Anil John Johnson, Sabulal Baby *

Phytochemistry and Phytopharmacology Division, Jawaharlal Nehru Tropical Botanic Garden and Research Institute, Pacha-Palode, 695562, Thiruvananthapuram, Kerala, India

ARTICLE INFO

Keywords:
Antiviral
Ayurveda
Charaka-Sushruta Samhitas
Jwara
Medicinal plants

ABSTRACT

Two of the earliest treatises in *Ayurveda*, the '*Charaka Samhita*' and the '*Sushruta Samhita*', describe numerous medicinal plants used in the treatment of *Jwara* (fever). Systematic studies carried out on these plants registered for '*Jwara*' are of high significance in antiviral drug development.

This article is a comprehensive review of the antiviral studies on medicinal plants listed for '*Jwara*' in '*Charaka-Sushruta Samhitas*', their antiviral entities and modes of action.

The botanical names of the medicinal plants used for '*Jwara*' were elucidated from their Sanskrit names in '*Charaka-Sushruta Samhitas*' and their subsequent interpretations. Antiviral studies on these plant species and their constituents were compiled from the literature retrieved from Scopus, PubMed, Google Scholar and other databases. Antiviral activities against various viruses were evaluated based on $EC_{50}/IC_{50}/LC_{50}$ values, high percent inhibitions and molecular docking parameters displayed by their extracts, secondary metabolites, short peptides, polyphenols, anthocyanins and polysaccharides. Their modes of action were also evaluated.

Strikingly, in antiviral studies very low $EC_{50}/IC_{50}/LC_{50}$ and high percent inhibitions were demonstrated by medicinal plants widely used as traditional medicines, vegetables, foods and flavours. Secondary metabolites (including essential oils), anthocyanins, polyphenols, short peptides and polysaccharides in these plants illustrated antiviral activities by hampering membrane permeability, cellular functions and replication cycle of harmful viruses.

Medicinal plants used for fever in *Ayurveda* could be used as natural sources of lead molecules for antiviral drug development. Antiviral activities displayed by these plants are justifying the ancient wisdom traditionally demonstrated over centuries.

1. *Ayurveda* and '*Jwara*'

Plants have been used for treatment of viral diseases in various traditional systems of medicine [1–3]. India has one of the oldest folk traditions; and the earliest references to the use of medicinal herbs are found in the Sanskrit literature [4,5]. The main literary sources of the Vedic era (1500 - 500 BCE) are the four *Vedas*: '*Rig Veda*', '*Yajur Veda*', '*Sama Veda*' and '*Atharva Veda*'. *Rig Veda, Yajur Veda* and *Atharva Veda* recorded 67, 82 and 288 medicinal plants, respectively. '*Ayurveda*' (considered as '*Upa Veda*' of '*Atharva Veda*') describes the properties of plant based drugs and their uses. The earliest treatise on '*Ayurveda*', '*Charaka Samhita*' ('Compendium of *Charaka*', ~900 BCE) written by Charaka is a great reference to diseases and medical procedures listing 341 plants and their products. '*Sushruta Samhita*' ('Compendium of *Sushruta*', ~600 BCE) which was written by Sushruta, a surgeon and teacher of '*Ayurveda*', is a more comprehensive and authoritative work of '*Ayurveda*' that contains illustrations of 1120 diseases, 700 healing plants and 121 preparations [5–9].

Ayurveda is focused on disease prevention and promotion of good health, by adopting a proper life style and assuming measures that rejuvenate the cells of the body [9,10]. It is based on the concepts of five elements ('*Panchabhuta*') *viz.*, '*Vayu*' (air), '*Jala*' (water), '*Prithvi*' (earth), '*Teja*' (fire), '*Akasha*' (space), which constitute the physical universe including the human body, and three '*doshas*' (meaning 'fault' or 'defect') *viz.*, '*Vata*', '*Pitta*' and '*Kapha*' (*Tridoshas*), which broadly refer to the functions of motion, digestion and cumulation [11–13]. In

Peer review under responsibility of Transdisciplinary University, Bangalore.
* Corresponding author.
E-mail address: sabulal@gmail.com (S. Baby).

https://doi.org/10.1016/j.jaim.2024.101085
Received 20 July 2024; Received in revised form 20 September 2024; Accepted 3 October 2024

other words, *Tridoshas* are the three psychobiological dimensions or biological rhythms harmonizing the functioning of the human body. The imbalance between the three '*doshas*' leads to diseases. The dominance of '*Vata*' dosh causes neurological disorders, manifested by poor blood circulation, anxiety, memory loss and related symptoms. '*Pitta*' imbalance gives rise to stomach troubles and variation in '*Kapha*' results in cholesterol related diseases. A disparity between '*Kapha*' and '*Vata*' doshas results in fever ('*Jwara*'). High 'Kapha' in the body contributes to cold and high 'Vata' lowers the digestive fire which results in indigestion, chills, and fatigue [12,13]. *Ayurveda* provides medicines of herbal origin to balance the '*doshas*', aiming to cure the diseases [14,15]. '*Jwara*', since it affects throughout the life, is considered as the 'lord of diseases'. *Ayurveda* also describes '*Jwara*' as the most dominant among diseases, affecting mind, body and the senses. High body temperature is regarded as the main characteristic of '*Jwara*' (fever) [16,17].

2. '*Jwara*': plants in *Charaka-Sushruta Samhitas*

Lifestyle disorders, stress, or incorrect nutrition cause the imbalance, leading to a dysfunctional system of digestion. Otherwise, toxins in the small and large intestines putrefy and spread to the entire body, and exposure to viruses leads to infection and fever. Several medicinal plants are mentioned in *Ayurveda* for fever-like symptoms. In this article, Sanskrit names of plants recorded in '*Charaka Samhita*' and '*Sushruta Samhita*' for treatment of '*Jwara*' (fever) are listed and their taxonomic names (including synonyms) were derived from various references. Tables S1 and S2 are listing these Sanskrit (alphabetically) and botanical names. There are 210 and 139 identified plant species listed for the healing of '*Jwara*' in '*Charaka Samhita*' and '*Sushruta Samhita*', respectively (Tables S1 and S2). The botanical identifications of the medicinal plants mentioned under '*Jwara*' are inconsistent due to their scribal variations and multiple species identities or synonyms [16]. On excluding repetitions, the total number plant species listed for '*Jwara*' in the two *Samhitas* is 250 (Tables S1 and S2).

These medicinal plants listed for '*Jwara*' are widely used as cure for fever and other diseases in various traditional systems of medicine [5–8]. In recent decades systematic phyto, biochemical, pharmacological and *in silico* studies elucidated the chemical entities and antiviral potentials of several of these medicinal plants. This article is the first comprehensive review of the antiviral studies on these traditionally used medicinal plants, their bioactive entities and underlying action mechanisms. The literature review of this article was last updated in September 2024.

3. Search strategy

Each plant species listed in Tables S1 and S2 was rigorously searched using the terms "botanical name" and "antiviral" in web-based resources such as Google Scholar, Scopus and PubMed, and retrieved data were analyzed. Synonyms of "botanical names" in Tables S1 and S2 were also searched for antiviral studies. These terms were searched in full texts of articles, including their title and abstract, and no date restrictions were applied. Full text of articles were obtained from open access resources (journals, databases), local libraries and from original authors of the studies.

4. Antiviral studies

We found antiviral studies only for 80 of these 250 species (Table 1, Table S3). Most of these plants subjected to antiviral studies are common edible species such as vegetable, cooking spices, aromatic spices and traditional medicines. The various examples are *Acorus calamus* L. (common name: sweet flag), *Aegle marmelos* (L.) Corrêa (wood apple), *Alpinia galanga* (L.) Willd (galangal), *Aerva lanata* (L.). Juss. (Kapurimadhuri), *Alhagi maurorum* Medik (camel thorn), *Alstonia scholaris* (L.). R.Br. (Indian devil tree), *Andrographis paniculata* (Burm. f.) Nees (green chireta), *Asparagus racemosus* Willd. (shatawari), *Azadirachta indica* A. Juss. (neem), *Barleria prionitis* L. (porcupine flower), *Boswellia serrata* Roxb. ex Colebr (Indian frankincense), *Centipeda minima* (L.). A.Braun & Asch (spreading sneezeweed), *Cinnamomum cassia* (L.). J.Presl (Chinese cinnamon), *Cissampelos pareira* L. (velvetleaf), *Cynodon dactylon* (L.) Pers. (Bermuda grass), *Citrus medica* L. (ganapati narakam), *Clitoria ternatea* L. (blue pea or butterfly pea), *Cocos nucifera* L. (coconut palm), *Coriandrum sativum* L. (coriander), *Cucumis melo* L. (muskmelon), *Curcuma longa* L. (turmeric), *Cymbopogon citratus* (DC.) Stapf (lemon grass), *Cyperus rotundus* L. (nut grass), *Eclipta prostrata* (L.) L. (false daisy), *Ficus benghalensis* L. (banyan), *Garcinia indica* (Thouars) Choisy (kokum), *Glycyrrhiza glabra* L. (licorice or sweetwood), *Hemidesmus indicus* (L.) R. Br. ex Schult. (Indian sarsaparilla), *Holarrhena pubescens* Wall. ex G.Don (Indrajao), *Hordeum vulgare* L. (barley), *Jasminum officinale* L. var. *grandiflorum* (jasmine), *Justicia adhatoda* L. (adalodakam), *Michelia champaca* L. (champa), *Mangifera indica* L. (mango), *Marsdenia tenacissima* (Roxb.) Moon (devil's tongue), *Momordica dioica* Roxb. ex Willd (spiny gourd), *Mucuna pruriens* (L.). DC. (velvet bean), *Nelumbo nucifera* Gaertn. (sacred lotus), *Nymphaea alba* L. (white water lily), *Ocimum basilicum* L. (basil), *Ocimum sanctum* L. (holy basil or tulsi), *Oroxylum indicum* (L.) Kurz (Indian trumpet tree), *Phyllanthus emblica* L. (Indian gooseberry or amla), *Phyllanthus niruri* L. (gale of the wind, keezhanelli), *Piper longum* L. (Indian long pepper or pippali), *Piper nigrum* L. (black pepper), *Piper retrofractum* Vahl (Javanese long pepper or Balinese long pepper), *Plumbago zeylanica* L. (white leadwort), *Pongamia pinnata* (L.) Pierre (malapari or karanja tree), *Punica granatum* L. (pomegranate or anar), *Putranjiva roxburghii* Wall. (lucky bean tree), *Ricinus communis* L. (castor bean), *Rubia cordifolia* L. (Indian madder), *Rhus parviflora* Roxb. (small flowered poison sumac), *Solanum nigrum* L. (black nightshade), *Sphaeranthus indicus* L. (East Indian globe thistle), *Swertia chirata* Buch.-Ham. ex Wall. (kiratatikta, chirayata), *Terminalia chebula* Retz. (chebulic myrobalan), *Thespesia populneoides* (Roxb.) Kostel. (Indian tulip tree), *Tinospora sinensis* (Lour.) Merr (Malabar gulbel), *Trachyspermum ammi* (L.). Sprague (ajwain, ajowan), *Vitis vinifera* L. (grape), *Withania somnifera* (L.) Dunal (ashwagandha or winter cherry), *Zingiber officinale* Roscoe (ginger), *Ziziphus jujuba* Mill. (Indian jujube, Indian plum)) (Table 1, Table S3). The systematic studies listed in Table 1, Table S3 are investigations on the antiviral activities of plant extracts, fractions, secondary metabolites, essential oils, short peptides, polysaccharides and their mechanisms of action. A notable number of studies attempted molecular docking and other *in silico* techniques towards determining the antiviral potential of molecules (ligands) of these plants traditionally used for '*Jwara*' in *Ayurveda* (Table 1, Table S3). The most promising antiviral leads discovered in *in-vitro/in-vivo* and *in silico* studies and their structures are listed in Table 1 and Fig. 1, respectively.

5. Antiviral leads

Table 1 is listing the entities of lead plants, which showed strong antiviral activities, indicated by very low $EC_{50}/IC_{50}/LC_{50}$ values, high % inhibitions and molecular docking (binding) parameters. *P. granatum* (pomegranate) rind water extract exhibited potent antiviral properties against HSV-1 and acyclovir-resistant HSV with EC_{50} values 0.56 and 0.02 μg/mL [18]. Ethanolic extract of *P. granatum* leaves treated on Vero cells infected with Zika virus-strains MR766 and HSV-2 showed antiviral activity (EC_{50}s 11.40, 3.29 μg/mL) [19]. Two fractions isolated from *N. alba* (white water lily) acetone extract restricted HCV NS3 gene expression in transfected target cells (EC_{50}s 37, 20 μg/mL) [20]. *C. citratus* (lemon grass) volatile oil, its nanoparticle and its hydrogel encapsulated nanoparticle showed EC_{50}s in HSV-1 inhibition as 11.59, 1.32 and 0.32 μg/mL, and their EC_{50}s against HSV-2 were 6.69, 1.34 and 0.33 μg/mL, respectively [21].

Table 1
Antiviral activity studies of medicinal plants listed for *Jwara* in *Charaka Samhita* and *Susruta Samhita*.

Sl. No.	Botanical name[a]	No.	Virus	Assay	Activity
[A] Secondary compounds					
1.	*Acorus calamus* L.	1	Dengue virus type 2 (DENV2)	Cytopathic inhibition (plaque, time-addition), lactate dehydrogenase assays	Tatanan A (**1**) isolated from *A. calamus* ethanol extract showed strong anti-DENV activity in DENV2-infected BHK-21 cells by alleviating CPE (EC_{50} 3.9 μM) [22]
2.	*Alpinia galanga* (L.) Willd.	1	Human immunodeficiency virus type 1 (HIV-1)	Quantification of HIV-1 p24 antigen in cell culture supernatant by ELISA	1′S-1′-acetoxychavicol acetate (ACA, **2**) isolated from the methanol extract of *A. galanga* rhizome inhibited HIV-1 replication. ACA (**2**) at 4 μM completely inhibited the export of RevNES fusion protein from the nucleus [23]
3.	*Andrographis paniculata* (Burm. f.) Nees	1	Herpes simplex virus type 1 (HSV-1)	Plaque reduction assay	Neoandrographolide (**3**) isolated from *A. paniculata* leaf ethanol extract showed the highest rate of anti-herpes activity on virus infected Vero cells (IC_{50} 7.97 μg/mL) [24]
		2	SARS-CoV-2	Plaque forming assay, qRT-PCR	Calu-3 and Vero E6 cells infected with SARS-CoV-2 treated with *A. paniculata* extract or andrographolide (**4**) for 48 h displayed dose-dependent inhibition of SARS-CoV-2 infection (IC_{50}s: Extract 0.036 μg/mL, andrographolide (**4**) 0.034 μM) [25]
		3	Respiratory syncytial virus (RSV)	Cytopathic inhibition assay	Andropanolide B (**5**) and andrographiside (**6**) isolated from 95% ethanolic extract of *A. paniculata* aerial parts showed significant reduction in CPE (IC_{50}s: Andropanolide B (**5**) 25 μg/mL, andrographiside (**6**) 30 μg/mL) [26]
4.	*Barleria prionitis* L.	1	Respiratory syncytial virus (RSV-A2 strain)	Cytopathic inhibition assay	3:1 combination of 6-*O*-*trans*-*p*-coumaroyl-8-*O*-acetylshanzhiside methyl ester (**7**) and 6-*O*-*cis*-*p*-coumaroyl-8-*O*-acetylshanzhiside methyl ester (**8**) isolated from the methanol soluble fraction of dichloromethane-isopropanol (1:1) extract of *B. prionitis* whole plant displayed significant anti-RSV activity (EC_{50} 2.46 μg/mL) [27]
5.	*Boswellia serrata* Roxb. ex Colebr.	1	Chikungunya virus (CHIKV-E2/E1), vesicular stomatitis virus G (VSV-G)	Pseudotyped lentiviral vector assays (CHIKV-E2/E1 and VSV-G pseudotyped vectors, luciferase assay (AAV-2 based vectors with CHIKV-luci, VSV-luci), immunofluorescence microscopy	Acetyl-11-keto-β-boswellic acid (ABA, **9**) displayed strong activity against CHIKV-E2/E1 and VSV-G pseudotyped vectors (IC_{50}s: CHIKV-E2/E1 6.75 μM, VSV-G 5.97 μM). 293T cells infected with CHIKV-luci or VSV-luci in presence of ABA (9) displayed significant decrease in viral infection (IC_{50}s: CHIKV-lu 4.51 μM, VSV-luci 2.30 μM) [28]
6.	*Centipeda minima* (L.) A.Braun & Asch.	1	Influenza virus A/Puerto Rico/8/34H1N1 (PR8)	CPE reduction, time of addition assays (co- and post-treatment assays)	Brevilin A (**10**) isolated from the supercritical extract of *C. minima* whole plant has demonstrated potent anti-influenza activity against the PR8 strain. It was found to be effective after virus entry into the cells and it displayed strong antiviral activity (IC_{50} 1.8 ± 0.6 μM, Selectivity index (SI) value 13.5) [29]
		2	Influenza A virus	Cytopathic reduction assay	Brevilin A (**10**) showed strong anti-influenza activity against various strains of viruses, including PR8, H1N1 (FM1), H3N2, and H9N2, (EC_{50}s: 2.96 ± 1.10, 1.60 ± 1.14, 3.28 ± 1.09, and 2.07 ± 1.12 μM) [30]
7.	*Curcuma longa* L.	1	Influenza virus strains A/Chicken/Korea/O1310/2001 (H9N2) and A/Sw/Kor/CAH1/04 (H1N1, KCTC 11165BP)	Influenza virus A (H1N1 and H9N2) neuraminidase inhibition, novel H1N1 (WT) and oseltamivir-resistant novel H1N1 (H274Y) neuraminidase inhibition assays	Curcumin (**11**), demethoxy curcumin (**12**) and bisdemethoxy curcumin (**13**) isolated from the ethanol extract of *C. longa* dried rhizomes showed strong inhibition of neuraminidases of H1N1 and H9N2 viral strains (IC_{50}s: H1N1 6.18 ± 0.64 to 40.17 ± 0.79 μg/mL, H9N2 3.77 ± 0.75 to 31.82 ± 1.33 μg/mL); 1,5-bis (4-hydroxyphenyl)-1,4-pentadiene-3-one (**14**) showed IC_{50}s of 6.18 and 3.77 μg/mL against influenza A H1N1 and H9N2 [31]
		2	Herpes simplex virus 1-strain KOS (HSV-1 strain KOS)	Cytopathic inhibition assay	Curcumin (**11**) and its derivatives, gallium-curcumin and cu-curcumin, on testing their effects on replication of HSV-1 in Vero cells showed significant antiviral activity (IC_{50}s: curcumin (**11**) 33.0 μg/mL, gallium-curcumin 13.9 μg/mL, cu-curcumin 23.1 μg/mL; SI values: curcumin 14.6, gallium-curcumin 18.4, cu-curcumin 14.1) [32]
		3	Influenza virus A/PR/8/34 (H1N1)	Cytopathic inhibition, determination of cytokines and chemokines by qRT-PCR and	Bisabola-3,10-dien-2-one (**15**), 4-(6-methyl-4-oxohept-5-en-2-yl)cyclohex-2-en-1-one (**16**)

(*continued on next page*)

Table 1 (*continued*)

Sl. No.	Botanical name[a]	No.	Virus	Assay	Activity
				bio-plex assays, proteomics and Western blotting, bioinformatic analysis	and 1,4-epidioxybisabola-2,10-dien-9-one (**17**) displayed significant inhibition of influenza virus-A/PR/8/34 (H1N1) replication in MDCK cells (IC_{50}s: Bisabola-3,10-dien-2-one (**15**) 23.1 μg/mL, 4-(6-methyl-4-oxohept-5-en-2-yl)cyclohex-2-en-1-one (**16**) 11.4 μg/mL, 1,4-epidioxybisabola-2,10-dien-9-one (**17**) 16.8 μg/mL) [33]
8.	*Eclipta prostrata* (L.) L.	1	Fish nodavirus, grouper nervous necrosis virus (GNNV)	MTT, cytopathic inhibition assays, RT-PCR	Dasyscyphin C (**18**) from *E. prostrata* treated with nodavirus infected SIGE cells showed viral inhibition (IC_{50}: 20 μg/mL) [34]
9.	*Garcinia indica* (Thouars) Choisy	1	HIV-1	HIV-1 RT-associated RNase H inhibition and RDDP inhibition assays, molecular docking study (OEDocking tool kit, OpenEye toolkit 2020.2.0)	Garcinol (**19**) showed significant inhibition of the wild-type HIV1-RNase H (IC_{50} 6.6 ± 2.1 μM) [35]
10.	*Glycyrrhiza glabra* L.	1	Hepatitis C virus (HCV)	Quantitative real time-PCR, transfection studies, Western blot	Glycyrrhizin (**20**) displayed dose-dependent antiviral activity in Huh-7 cells infected with HCV (IC_{50}: 14 ± 2 μg). Cells treated with 10 IU of IFN-alpha 2b and 10 μg/mL of glycyrrhizin (**20**) displayed synergistic effect with 95% reduction in viral titer [36]
11.	*Hemidesmus indicus* (L.) R. Br. ex Schult.	1	HIV-1	*In vitro* HIV-1 reverse transcriptase (RT)-associated ribonuclease H (RNase H) inhibition, HIV-1 RT-associated RNA-dependent DNA polymerase (RDDP), cellular α-glucosidase inhibition assays	*H. indicus* dried root powder decoction and lupeol (**21**) showed significant activity (IC_{50}s: 2.9 μM, 11.6 μM). The root powder decoction showed strong inhibition of RDDP (IC_{50} 7.5 μM) [37]
12.	*Jasminum officinale* L. var. *grandiflorum*	1	Hepatitis B virus (HBV-transfected human HepG2 cell line), duck hepatitis B virus (DHBV)	ELISA for extracellular hepatitis B antigen (HBeAg) and hepatitis B surface antigen (HBsAg), dot blot analysis, DHBV challenged duckling model	Oleuropein (**22**) inhibited HBsAg secretion from HBV transfected HepG2 2.2.15 cells dose-dependently (IC_{50} 23.2 μg/mL) [38]
		2	Hepatitis B virus (HBV), duck hepatitis B virus (DHBV)	ELISA for extracellular hepatitis B antigen (HBeAg) and hepatitis B surface antigen (HBsAg), dot blot analysis, DHBV challenged duckling model	HBV transfected HepG2 2.2.15 cells treated with 8-*epi*-kingiside (**23**) displayed significant reduction of HBsAg secretion dose-dependently (IC_{50}: 19.4 μg/mL) [39]
13.	*Marsdenia tenacissima* (Roxb.) Moon	1	HIV-1 (transfected to SupT1 cells)	HIV inhibition (luciferase assay)	Marstenacisside D7 (**24**) and marstenacisside E6 (**25**) showed 81.3% and 80.9% inhibition of HIV-1, respectively [40]
14.	*Nelumbo nucifera* Gaertn.	1	HIV-1 (IIIB isolate)	p24 antigen ELISA assay	Liensinine (**26**), neferine (**27**) and isoliensinine (**28**) showed strong anti-HIV-1 activity (EC_{50}s < 0.8 μg/mL), and nuciferine (**29**) showed anti-HIV activity at EC_{50} 0.8 μg/mL [41]
15.	*Ocimum basilicum* L.	1	Herpes virus (HSV-1, 2), adenovirus (ADV-3, 8, 11), hepatitis B surface antigen (HBsAg) and hepatitis B e antigen (HBeAg), coxsackievirus B1 (CVB1), enterovirus 71 (EV71)	XTT, anti-HBV assays	Ursolic acid (**30**) showed the strongest activity against HSV-1 (EC_{50}: 6.6 μg/mL; selectivity index (SI) 15.2), ADV-8 (EC_{50}: 4.2 μg/mL; SI 23.8), CVB1 (EC_{50}: 0.4 μg/mL; SI 251.3) and EV71 (EC_{50}: 0.5 μg/mL; SI 201). Apigenin (**31**) demonstrated the highest activity against HSV-2 (EC_{50}: 9.7 μg/mL; SI 6.2), ADV-3 (EC_{50}: 11.1 μg/mL; SI 5.4), hepatitis B surface antigen, HBsAg (EC_{50}: 7.1 μg/mL; SI 2.3) and hepatitis B e antigen, HBeAg (EC_{50}: 12.8 μg/mL; SI 1.3). Linalool (**32**) showed strongest activity against ADV-11 (EC_{50}: 16.9 μg/mL; SI 10.5) [42]
16.	*Phyllanthus emblica* L.	1	Coxsackie virus B3 (CVB3)	Cytopathic inhibition assay	Phyllaemblicin B (**33**) and phyllaemblicin C (**34**) exhibited strong anti-CVB3 activity (CC_{50}s: 50.2 μg/mL, 67.7 μg/mL; IC_{50} 7.8 μg/mL, 11.0 μg/mL) [43]
17.	*Phyllanthus niruri* L.	1	Duck hepatitis B virus (DHBV)	Fluorescence quantitative PCR (FQ-PCR)	Treatment of HepG2.2.15 cells with niranthin (**35**) at various concentrations for 4 days resulted in significant reduction of HBsAg and HBeAg secretion in a dose-dependent manner (IC_{50}s: 15.6 μM, 25.1 μM) [44]
		2	Human hepatitis B virus	MTT assay, determination of HBsAg and HBeAg, FQ-PCR, short-term toxicity assay	In human HBV-transfected liver cell line HepG2.2.15, nirtetralin B (**36**) suppressed the secretion of HBV antigens dose-dependently (IC_{50}s: 17.4 μM (HBsAg), 63.9 μM (HBeAg)) [45]
18.	*Punica granatum* L.	1	Herpes simplex virus-2 (HSV-2)	Cytopathic inhibition assay, docking analysis (docking server software tool, drug likeness by PreADMET online web based software)	Punicalagin (**37**) isolated from the ethanolic extract of *P. granatum* fruit peel at 31.25 μg/mL displayed 100% anti HSV-2 activity. In docking analysis with the protein targets of HSV-2, punicalagin (**37**) showed significant inhibition of the protein targets with a low binding energy of −11.97 kcal/mol [46]

(*continued on next page*)

Table 1 (*continued*)

Sl. No.	Botanical name[a]	No.	Virus	Assay	Activity
		2	Human herpes virus-3 (HHV3) (Chickenpox and herpes Zoster)	Cytopathic inhibition assay, docking analysis (with discovery Studio version 4.0 and drug likeness by ADMETSAR software)	*P. granatum* leaf aqueous extract showed significant anti-HHV3 activity. MIC values of the aqueous extract on HHV-3 from Chickenpox and herpes Zoster were 15.62 and 31.25 μg/mL, respectively. In docking analysis apigenin (**31**), isoquercetin (**38**) and luteolin (**39**) displayed binding energies of −318.30, −220.01 and −219.61 kcal/mol, respectively [47]
		3	HIV-1	RNase H polymerase independent cleavage, Homogeneous time-Resolved Fluorescence (HTRF) IN LEDGF-dependent assays	Punicalagin (**37**), punicalin (**40**) and ellagic acid (**41**) displayed strong inhibition of HIV-1 RT-associated RNase H function (IC_{50}s: 0.12 μM, 0.18 μM, 1.4 μM) and HIV-1 integrase LEDGF-dependent activities (IC_{50}s: 0.065 μM, 0.09 μM, 0.075 μM) *in vitro*. Luteolin (**39**) and apigenin (**31**) showed inhibition of RNase H and IN functions (IC_{50}s: 3.7–22 μM), whereas luteolin-7-*O*-glucoside (**42**) displayed selective inhibition of HIV-1 IN [48]
19.	*Rubia cordifolia* L.	1	Hepatitis B virus (HBV)	HBsAg enzyme immunoassay (EIA)	Furomollugin (**43**) and mollugin (**44**) significantly suppressed the secretion of hepatitis B surface antigen (IC_{50}s: 2.0 μg/mL, both) [49]
20.	*Swertia chirata* Buch.-Ham. ex Wall.	1	Human immunodeficiency virus-1 (HIV-1), HIV-2, Simian immunodeficiency virus (SIV)	Viral protein R (Vpr) expression assay	Chloroform extract of *S. chirata* whole plant, bellidifolin (**45**) and oleanolic acid (**46**) at 10 μM dose showed 128, 116 and 168% inhibition of Vpr expression [50]
21.	*Terminalia chebula* Retz.	1	Herpes simplex virus-2 (HSV-2)	Plaque reduction (direct, post infection, attachment and penetration of viral assays)	Ethanolic extract (50%) from *T. chebula* fruits, chebulagic acid (**47**) and chebulinic acid (**48**) showed significant direct HSV-2 inhibitory activity (IC_{50}s 0.01 μg/mL, 1.41 μg/mL, 0.06 μg/mL) on Vero cells. Extract and compounds strongly inhibited the binding of HSV-2 to Vero cells dose-dependently (IC_{50}s: 0.48 μg/mL, 1.66 μg/mL, 0.29 μg/mL) [51]
		2	Hepatitis C virus (HCV)	HCV protease inhibition assay	Casuarinin (**49**), pentagalloyl glucose (**50**) and chebulagic acid (**47**) isolated from *T. chebula* fruit methanol extract showed significant HCV protease inhibitory activity (IC_{50}s: 9.6 μM, 10.6 μM, 5.2 μM) [52]
		3	HIV-1	HIV-1 integrase, reverse transcriptase inhibition assays	Gallic acid (**51**) and three galloyl glucoses (1,3,6 tri-*O*-galloyl-β-D-glucopyranose (**52**), 1,2,3,4,6-penta-*O*-galloyl-β-D-glucopyranose (**53**), chebulagic acid (**47**)) isolated from the ethyl acetate fraction of *T. chebula* fruit aqueous extract displayed HIV-1 integrase inhibitory activity (IC_{50} 13.7–19.7 μM), while in reverse transcriptase inhibitory assay chebulagic acid (**47**) only showed significant inhibitory action (IC_{50} 20.6 μM) [53]
22.	*Zingiber officinale* Roscoe	1	Rhinovirus IB (RVIB)	Plaque reduction assay	β-Sesquiphellandrene (**54**) isolated from *Z. officinale* rhizomes when treated on HeLa cells infected with RVIB displayed significant activity (IC_{50} 0.44 μM) [54]
23.	*Ziziphus jujuba* Mill.	1	Influenza A/PR/8 virus	Cytopathic inhibition assay (SRB method), influenza A/PR/8 virus challenged C57BL/6 mice model	Betulinic acid (**55**) isolated from *Z. jujuba* roots treated on A549 human lung adenocarcinoma epithelial cell infected with A/PR/8/34 virus displayed 98% inhibition at 50 μM and 30% inhibition at 10 μM [55]
		2	Porcine epidemic diarrhea virus (PEDV)	Cytopathic inhibition assay	Jubanine H (**56**) and nummularine B (**57**) isolated from the methanol extract of *Z. jujuba* roots displayed inhibition of PEDV in Vero cells (EC_{50}s: 4.49 μM, 6.17 μM) [56]
[B] Secondary compounds (*in silico*)					
24.	*Alpinia galanga* (L.) Willd.	1	SARS-CoV-2	Molecular docking (using MOE 2010, ChemDraw software, PDB resources)	Galangin (**58**) showed strong inhibitory activity against SARS-CoV-2 protease domain (6LU7), spike glycoprotein (6LXT) and RBD-ACE2 (6VW1) with Gibbs free energies −12.96, −7.89, −7.60 kcal/mol, respectively. Docking scores of 1′S-1′-acetoxychavicol acetate (ACA) (**2**) to these three protein targets were −9.94, −6.05 and −6.16 kcal/mol, respectively [57]
25.	*Alstonia scholaris* (L.) R.Br.	1	SARS-CoV-2	Molecular docking (using algorithms in LibDock protocol of BIOVIA discovery Studio and Auto Dock Vina)	Akuammicine N-oxide (**59**) of *A. scholaris* showed inhibition of main protease of SARS-CoV-2 with highest M^{pro} binding energy

(*continued on next page*)

Table 1 (*continued*)

Sl. No.	Botanical name[a]	No.	Virus	Assay	Activity
					(binding energy −8.4 kcal/mol, Libdock score 147.92 kcal/mol) [58]
26.	*Andrographis paniculata* (Burm. f.) Nees	1	SARS-CoV-2	Molecular docking (using autodock vina, drug databank resources), molecular dynamics simulation (using CHELPG approach)	Neoandrographolide (**3**) displayed significant binding affinity to 3CLpro, PLpro, RdRp and spike-ACE2 complex (binding free energy: −31.4, −28.5, −17.1, −23.9 kcal/mol) [59]
		2	Dengue virus (DENV-2 TR-1751)	RT-PCR, molecular docking (using Auto Dock V4.2.6 software)	Andrographolide (**4**) showed 97.2% inhibition at 15.62 μg/mL of maximum nontoxic dose (MNTD) against DENV-2. Andrographolide (**4**) showed significant interaction with DENV-2-NS5 receptor protein at Tyr89, Met116, Met116, Met116 and Ser12 residues (total binding energy: −7.35 kcal/mol) [60]
		3	Zika virus (ZIKV)	Molecular docking studies (using AutoDock 4.2.6, MetaPocket 2.0, SWISS ADME website, pkCSM prediction database)	Bisandrographolide A (**60**) (−11.7 kcal/mol), andrographolide (**4**) (−10.2 kcal/mol) and andrographiside (**6**) (−9.7 kcal/mol) showed significant binding affinities to NS2B-NS3 protease [61]
		4	Swine flu virus (H1N1 virus)	Molecular docking studies (using Autodock4.2, CASTp & Q-Site finder, ModWeb online server, NCBI PubChem compound database)	Andrographolide (**4**) displayed strong inhibition of neuraminidase (A/Blore/NIV236/2009(H1N1)) by structural conformation changes in the 150 loop (binging energy: −10.88 kcal/mol, total intermolecular energy: −12.07 kcal/mol, bioactivity value (Ki): 10.59 nmol/L) [62]
27.	*Asparagus racemosus* Willd.	1	SARS-CoV-2	Molecular docking (using Schrodinger Glide SP module, PDB IDs, AMBER18 software package, ligands parameterized with ANTECHAMBER)	MM-GBSA based binding free energy calculations with respect to SARS-CoV-2 spike receptor showed maximum with asparoside-D (**61**) (ΔG_{bind} of −66.49 kcal/mol) followed by asparoside-C (**62**) (ΔG_{bind} −62.61 kcal/mol), and SARS-CoV-2 NSP15 endoribonuclease bound to compounds showed maximum free energy with asparoside-C (**62**) (ΔG_{bind} −51.42 kcal/mol), followed by asparoside-F (**63**) (ΔG_{bind} - 55.30 kcal/mol) and asparoside-D (**61**) (ΔG_{bind} −72.46 kcal/mol) [63]
28.	*Azadirachta indica* A. Juss.	1	Hepatitis C virus (HCV)	Molecular docking (MOE software with LigX option)	3-Deacetyl-3-cinnamoyl-azadirachtin (**64**) displayed strong affinity to bind the active site of NS3/4 protease (minimum S-score: −29.20) [64]
29.	*Boerhavia diffusa* L.	1	SARS-CoV-2	Molecular docking (Auto dock tool, Lamarckian genetic algorithm, RCSB protein databank, ADME studies; drug likeness prediction by ADME [a] T using pkCSM pharmacokinetics tool)	Biorobin (**65**), bioquercetin (**66**) and boerhavisterol (**67**) are strong inhibitors of SARS-CoV-2 main proteases (binding energy: 8.17 kcal/mol, - 7.97 kcal/mol, - 6.77 kcal/mol) [65]
30.	*Boswellia serrata* Roxb. ex Colebr.	1	SARS-CoV-2	Molecular docking (Autodock 4.2 for docking analysis, ADME determined by Swiss ADME tool)	Euphane (**68**), ursane (**69**), α-amyrin (**70**) and 2,3-dihydroxyurs-12-en-28-oic acid (71) showed significant Mpro inhibition (binding energies: −10.47 kcal/mol, −10.41 kcal/mol, -9.99 kcal/mol, −9.72 kcal/mol) [66]
31.	*Citrus medica* L.	1	SARS-CoV-2	Molecular docking (Schrodinger suite, protein preparation wizard in the Maestro software, PDB resources)	Rhoifolin (**72**) (−7.36) and neohesperidin (**73**) (−9.94) showed highest glide score, and neohesperidin (**73**) (−60.95 kcal/mol) and hesperidin (**74**) (−59.87 kcal/mol) displayed highest binding free energies, respectively, on SARS-CoV-2 protein targets like spike protein and ACE-2 [67]
32.	*Cocos nucifera* L.	1	SARS-CoV-2	Molecular docking (MOE software)	Jezonofol (**75**) isolated from *C. nucifera* endocarp showed the highest potency towards PLpro (binding energy: −60.7 kcal/mol) [68]
33.	*Cyperus rotundus* L.	1	SARS-CoV-2	Molecular docking (g LibDock module, discovery Studio, protein data Bank resources, molecular dynamics simulation by GROMACS version 2019.4, ADMET prediction by pkCSM tool)	Lupeol (**21**) exhibited maximum affinity to the target protein with a CDOCKER energy of −70.04 kcal/mol. In ADMET analysis, β-amyrin (**76**) and stigmasta-5,22-dien-3-ol[b] (**77**) demonstrated superior anti-SARS-CoV-2 activity [69]
34.	*Glycyrrhiza glabra* L.	1	SARS-CoV-2	Molecular docking (AutoeDock Vina, drug likeness prediction and ADMET properties prediction by OSIRIS property explorer and admetSAR webserver)	Glycyrrhizic acid[c] (**20**) from *G. glabra* in docking evaluation against the main protease (Mpro-PDB ID-6Y2E) of SARS-CoV-2 showed strong inhibition (binding affinity: −8.0 kcal/mol). Glabridin (**78**) exhibited binding energy of −7.3 kcal/mol [70]
35.	*Justicia adhatoda* L.	1	SARS-COV-2	COVID-19 docking Server	Anisotine (**79**) showed highest inhibitory activity on protease and RdRp with binding energies of −7.8 and −9.2 kcal/mol, respectively. Vasicoline (**80**) exhibited

(*continued on next page*)

Table 1 (*continued*)

Sl. No.	Botanical name[a]	No.	Virus	Assay	Activity
					significant inhibition of RdRp with binding energy of −8.5 kcal/mol but it displayed only moderate inhibition of protease with binding energy of −7.0 kcal/mol [71]
		2	SARS-CoV-2	Molecular docking (AutoDock Vina, PubChem database server, RCSB protein data Bank, Swiss ADME online server, Schrodinger suite for MM-GBSA analysis)	Anisotine (**79**) showed significant inhibition against SARS-CoV-2 Mpro (binding energy: −7.9 kcal/mol) [72]
		3	SARS-CoV-2	Molecular docking (AutoDock, Schrodinger, Biovia Computer aided drug design approach, PDB resources)	Adhatodine (**81**) and vasnetine (**82**) showed significant binding affinity against SARS-CoV-2 target proteins (binding energy: −9.60 kJ/mol, −8.78 kJ/mol) [73]
36.	*Michelia champaca* L.	1	SARS-CoV-2	Molecular docking (AutoDock software, RSCB Protein Data Bank, PubChem resources)	Taraxerol (**83**), taraxerone (**84**), ferulic acid (**85**) and gallic acid (**51**) in molecular docking analysis with ACE2 receptor displayed their capability to bind the active sites of the receptor protein (binding energy: −9.6 kcal/mol, −9.4 kcal/mol, −6.2 kcal/mol, −5.6 kcal/mol) [74]
37.	*Mimosa pudica* L.	1	Herpes simplex virus type I (HSV-1)	Molecular docking (Autodock Vina, discovery Studio 3.5 Visualizer, online databases: PubMed, PubChem, PDB)	Orientin (**86**) and isovitexin (**87**) displayed significant binding with HSV-1 thymidine kinase protein (docking score: −7.9 kcal/mol, −7.7 kcal/mol) [75]
38.	*Momordica dioica* Roxb. ex Willd.	1	SARS-CoV-2	Molecular docking (with AutoDock 4.2.6, AutoDock Vina, PubChem database, metaPocket server, SwissADME software), *in vitro* protein inhibition assay	Oleanolic acid (**46**) showed highest affinity to main SARS-CoV-2 protease (−8.5 kcal/mol), RdRp (−8.3 kcal/mol), spike protein with ACE2 receptor (−8.5 kcal/mol) and MERS-CoV with hDPP4 receptor (−8.2 kcal/mol). In *in vitro* protein inhibition assay, Mpro-3CL protease, DPP4, recombinant spike S1 & S2 (S-ECD) protein and RdRp were incubated with 0.005–1 mM of catechin (**88**), quercetin (**89**), hederagenin (**90**) and oleanolic acid (**46**); quercetin (**89**) displayed highest inhibition of main protease (IC_{50}: 0.062 μM) and spike protein (IC_{50}: 0.052 μM), and catechin (**88**) displayed highest inhibition of RdRp (IC_{50}: 0.712 μM) and DPP4 protein (IC_{50}: 0.032 μM) [76]
39.	*Oroxylum indicum* (L.) Kurz	1	SARS-CoV-2	Molecular docking (with Autodock Vina, discovery Studio 2020 Client and PyMol softwares, ADME analysis by pkCSM, protein data bank, PubChem database)	Molecular docking analysis of selected ligands from *O. indicum* with the main protease of SARS-CoV-2 displayed significant binding affinity with Mpro (binding energy: Baicalein-7-*O*-diglucoside (**91**) −9.1 kcal/mol, chrysin-7-*O*-glucuronide (**92**) −8.6 kcal/mol, oroxindin (**93**) −8.1 kcal/mol, scutellarein (**94**) −8.0 kcal/mol) [77]
40.	*Piper longum* L.	1	SARS-CoV-2	Molecular docking (Auto Dock Vina software, Pyrx docking software, PDB database, Biovia discovery Studio Visualizer software, PubChem, ADMET property analysis by SWISS-ADME software)	I-Asarinin (**95**) displayed best binding affinity score of −10.8 kcal/mol against SARS-CoV-2 papain-like protease [78]
		2	SARS-CoV-2	Molecular docking (AutoDock program version 4.2, Autodock tools (ADT) version 1.5.6, PDB database)	Piperundecalidine (**96**) showed high binding energy of −9.54 kcal/mol against SARS-CoV-2 main protease (Mpro) [79]
41.	*Piper nigrum* L.	1	SARS-CoV-2	Molecular docking	Piperine (**97**) showed high binding affinity (−7.0 kcal/mol) to the RNA-binding pocket of the nucleocapsid [80]
42.	*Terminalia chebula* Retz.	1	Hepatitis C virus (HCV NS3/4A)	Molecular docking and network pharmacology (AutoDock Vina, STRING and Reactome pathway databases, Cytoscape 3.6.1, MolSoft, ADVERpred, PreADMET)	Chebulagic acid (**47**) and 1,2,3,4,6-pentagalloyl glucose (**50**) displayed significant HCV NS3/4A inhibitory activity (binding energy: −8.6 kcal/mol, −7.7 kcal/mol) [81]
43.	*Tinospora sinensis* (Lour.) Merr.	1	SARS-CoV-2	Molecular docking analysis (Autodock-Pyrx tool, AutoDock Vina, NCBI Pubchem database)	In docking analysis with SARS-CoV-2 main protease, isocolumbin (**98**) from *T. sinensis* displayed significant inhibition of the main protease (binding energy: −8.6 kcal/mol) [82]
44.	*Vigna mungo* (L.) Hepper	1	SARS-CoV-2	Molecular docking (AutoDock Vina, PyMOL, discovery Studio, Pubchem, PDB)	In molecular docking analysis of *V. mungo* ligands against the SARS-CoV-2 3C-like protease, kievitone (**99**), glycinol (**100**), isoferreirin (**101**), stigmasterol (**77**)[b], β-sitosterol (**102**), and campesterol (**103**) displayed binding energies as −7.9, −7.5, −7.4, −7.9, −7.3 and −7.5 kcal/mol, respectively [83]

(*continued on next page*)

Table 1 (*continued*)

Sl. No.	Botanical name[a]	No.	Virus	Assay	Activity
45.	*Vigna radiata* (L.) R.Wilczek	1	SARS-CoV-2	Ligand molecular docking studies	Naringin (**104**) and neohesperidin (**73**) showed strong inhibition against SARS-CoV-2 3C-like protease (binding energy: −7.8 kcal/mol, −8.3 kcal/mol) [83]
46.	*Withania somnifera* (L.) Dunal	1	SARS-CoV-2	Virtual screening, *in silico* evaluation	Withanolides A (**105**) and B (**106**) showed binding energies of −10.13 and −10.21 kcal/mol with human ACE2 receptor and −9.78 and −9.4 kcal/mol with SARS-CoV spike glycoprotein [84]
47.	*Zingiber officinale* Roscoe	1	SARS-CoV-2	Molecular docking (discovery Studio Visualizer, Autodock 4.2, Cygwin, PDB database, ADME analysis with SwissADME software)	In molecular docking analysis gingerenone A (**107**) from *Z. officinale* demonstrated significant inhibition of the SARS-CoV-2 target proteins (6LU7, 7JTL) (binding energy: −4.8 kcal/mol, −7.65 kcal/mol) [85]
		2	SARS-CoV-2	Molecular docking and dynamics (Maestro Schrödinger 2020-3 software), SARS-CoV-2 3CL protease *in vitro* inhibition assay	In molecular docking studies, spinasterone (**108**) from *Z. officinale* displayed highest binding energy of −87.41 kcal/mol against SARS-CoV-2 3CL protease. In *in vitro* SARS-CoV-2 3CL protease inhibition assay, 24-methylcholesta-7-en-3β-on (**109**) showed 75% inhibition of the 3CL protease (binding energy: −68.80 kcal/mol) [86]
[C] Extracts					
48.	*Alhagi maurorum* Medik.	1	Foot and mouth disease virus (FMDV)	Cytopathic inhibition assay	Methanol extract (80%) of *A. maurorum* aerial parts displayed potent cytopathic effect (CPE) at 3 μg/mL against FMDV infected RBK cells [87]
49.	*Andrographis paniculata* (Burm. f.) Nees	1	Dengue virus −1 (DENV-1)	Cytopathic inhibition, plaque inhibition assays	Methanolic extract of *A. paniculata* aerial parts at its MNTD (20 μg/mL) and ½MNTD displayed anti-DENV-1 inhibitory activity (inhibition of CPE formation) in HepG2 cells [88]
50.	*Cinnamomum cassia* (L.) J.Presl	1	Human respiratory syncytial virus (HRSV)	Plaque reduction, viral syncytium assays, Western blot analysis of viral fusion protein synthesis	Hot water extract of dried twigs of *C. cassia* showed strong antiviral activity against HRSV infection in HEp-2 and A549 cells, near-completely inhibiting plaque formation at 30 μg/mL (IC_{50}s: HEp-2 cells 7.2 μg/mL, A549 cells 6.8 μg/mL) [89]
51.	*Cissampelos pareira* L.	1	DENV-1 (Nauru Island, U88535), DENV-2 (new Guinea C, AF038403), DENV-3 (H87, M93130), DENV-4 (Dominica, M14931)	Plaque reduction assay, plaque reduction neutralization test (pre-incubation test), DENV-2 challenged AG129 mouse model	Antiviral activity of alcoholic extract of *C. pareira* aerial parts (cipa) was highest against DENV-2 (IC_{50}: 1.97 μg/mL) and DENV-4 (IC_{50}: 1.23 μg/mL), while DENV-1 and DENV-3 showed relatively low activity (IC_{50}s: DENV-1 11.11 μg/mL, DENV-3 3.17 μg/mL) [90]
		2	Dengue virus, SARS-CoV-2	TaqMan Real-time RT-PCR assay	Whole plant aqueous extract showed 98% inhibition of SARs-COV-2 replication in infected Vero cell cultures [91]
52.	*Cocos nucifera* L.	1	Acyclovir-resistant herpes simplex virus type 1 (ACVr-HSV-1)	Cytopathic inhibition assay, quantification of viral titre	Fraction II demonstrated selective toxicity to HEp-2 cells and higher antiviral activity than the crude water extract of coconut husk fiber (virucidal Index: HEp-2 cells 1.0, 1.81; Vero cells 3.25 and 3.0) [92]
53.	*Curcuma longa* L.	1	Dengue virus (DENV-2)	Antiviral focus assay, DENV-2 infected Huh7it-1 cells challenged ddY mice model	*C. longa* extract (containing 19% curcuminoids) treated on DENV-2 before infecting the Huh7it-1 cells showed inhibition of DENV-2 concentration dependently, and 100% viral inhibition was observed at 80 μg/mL (IC_{50}: 17.91 μg/mL) [93]
		2	Hepatitis C virus (HCV)	Anti-HCV activity by virus titration and immunostaining, docking analysis (using ChemBioOffice program Ultra 11.0, Molegro virtual docking ver 5.5 program ver 5.5)	*C. domestica* (synonym) rhizome ethanol extract showed strong anti-HCV activity (IC_{50}: 1.68 μg/mL) [94]
		3	Polio virus	Cytopathic inhibition (pre/post infection) assay, determination of virus-induced syncytia	*C. longa* methanol extract inhibited polio virus at the maximum non-toxic concentration (MNTC) of 0.03 μg/mL (IC_{50}: 0.07 μg/mL, SI: 2.16) [95]
54.	*Nelumbo nucifera* Gaertn.	1	Herpes simplex virus type 1 (HSV-1), TK-HSV-1 strain	Plaque reduction, electrophoretic mobility shift assays, PCR, Western blot	Ethanolic extract (NN, 100 μg/mL) of *N. nucifera* seeds, its fraction (NN–B, 50 μg/mL) and subfraction (NN–B-5, 50 μg/mL) displayed significant anti-HSV-1 activity in HeLa cells. Sub-fraction showed dose dependent anti-HSV activity (IC_{50}: 21.3 μg/mL) [96]
55.	*Phyllanthus niruri* L.	1	Hepatitis C virus (HCV)	Anti-hepatitis C activity assay	*P. niruri* ethanol extract evaluated for its anti-HCV activity in Huh 7it-1 cells revealed strong inhibition (IC_{50}: 4.14 μg/mL) [97]

(*continued on next page*)

Table 1 (*continued*)

Sl. No.	Botanical name[a]	No.	Virus	Assay	Activity
56.	*Punica granatum* L.	1	Influenza virus A/Puerto Rico/8/34 (H1N1; PR8)	Cytopathic inhibition (MTT), hemagglutination assays	Crude ethanolic extract of *P. granatum* peel, its ethyl acetate and n-butanol fractions treated on MDCK cells infected with influenza virus A (H1N1) showed strong antiviral activity (IC_{50}s: 6.45 μg/mL, 5.60 μg/mL, 6.07 μg/mL) [98]
		2	Mosquito-borne Mayaro virus	Plaque inhibition, immunofluorescence assays, transmission electron microscopy (TEM)	*P. granatum* ethanol extract and its fraction containing punicalagin (**37**) treated on Vero cells infected with Mayaro virus displayed significant antiviral activities (IC_{50}s: 12.3 μg/mL, 29.9 μg/mL) [99]
		3	Adenovirus type 5	Cytopathic inhibition (MTT) assay	Ethanol extract of *P. granatum* dried peels treated on HeLa cells infected with adenovirus (type 5) displayed complete inhibition of CPE at 30 μg/mL (IC_{50}: 18.6 ± 6.7 μg/mL) [100]
		4	Arthropod-borne Mayaro virus (MAYV)	Plaque inhibition, virus yield inhibition assay	Ethanol extract of *P. granatum* shell and punicalagin (**37**) treated on Vero cells infected with MAYV displayed significant antiviral activity (IC_{50}s: 12.3 μg/mL, 28.2 μg/mL) [101]
		5	Herpes simplex virus-1 (HSV-1), aciclovir-resistant HSV (HSV-ACR)	Plaque reduction assay	*P. granatum* rind extract (PRE) exhibited potent antiviral properties against HSV-1 and aciclovir-resistant HSV (EC_{50}s: 0.56 μg/mL, 0.02 μg/mL) [18]
		6	Zika virus (strains MR766 and HPF2013), herpes simplex virus-2 (HSV-2), vaccinia virus (VACV)	Plaque reduction, immunofluorescence, binding, time-of-addition assays	Leaf ethanolic extract of *P. granatum* treated on Vero cells infected with Zika virus-strains MR766 and HSV-2 showed antiviral activity (EC_{50}s: 11.40 μg/mL, 3.29 μg/mL). In plaque reduction assays on Vero cells infected with ZIKV- MR766 and HPF2013 strains ellagic acid (**41**) displayed anti-ZIKV activity (EC_{50}s: 0.86 μM, 46.23 μM) [19]
57.	*Thespesia populneoides* (Roxb.) Kostel.	1	Herpes simplex virus-1 & 2, vaccinia, vesicular stomatitis, coxsackie, respiratory syncytical, feline corona, feline herpes, parainfluenza, reo virus-1, sindbis, punta toro viruses	Cytopathy inhibition assay	Methanolic extract of *T. populneoides* flowers displayed significant antiviral activity on HeLa cells infected with vesicular stomatitis, coxsackie and respiratory syncytical viruses (EC_{50}: 20 μg/mL) [102]
58.	*Vitis vinifera* L.	1	SARS-CoV-2, HSV-1	Plaque inhibition, gene expression assays	*V. vinifera* leaf extract at 10 μg/mL inhibited both HSV-1 and SARS-CoV-2 replication in the early stages of infection on Vero cells (ATCC CCL-81) by directly blocking the proteins enriched on the viral surface [103]
[D] Polysaccharide fractions					
59.	*Cucumis melo* L.	1	Herpes simplex virus 1 (HSV-1)	Plaque reduction assay (MTT assay)	Sulfated derivative of pectin extracted from *C. melo* pulp (SPCm) exhibited antiviral activity against ACV-sensitive (KOS) and ACV-resistant (AR-29) strains of HSV (IC_{50}s: 6 μg/mL, 12 μg/mL) [104]
60.	*Hordeum vulgare* L.	1	Human influenza A/H3N2 virus (A/Novosibirsk/RII-27192S/2020 (H3N2) strain)	*In vitro* microinhibition (MTT), hemagglutination (HA) inhibition assays	Polysaccharide rich fraction from the brans of *H. vulgare* (HVWP) showed significant inhibition of viral growth in MDCK cells (IC_{50}: 23.73 μg/mL) [105]
61.	*Nelumbo nucifera* Gaertn.	1	HIV-1	RT inhibitory activity against a purified recombinant HIV-1 RT using the cell-free RT colorimetric kit	Macromolecular polysaccharide-protein complex obtained from *N. nucifera* rhizomes inhibited RT and HIV-1 3′-processing (IC_{50}s: 33.7 μM, 5.28 μM) [106]
[E] Peptide fraction					
62.	*Mucuna pruriens* (L.) DC.	1	Hepatitis C virus (HCV)	Cytopathic inhibition assay	Peptide fraction (5–10 kDa) obtained from *M. pruriens* beans treated on human hepatoma cell line (HEp-2) infected with HCV displayed significant antiviral activity (IC_{50}: 19.40 μg/mL) [107]
[F] Essential oils, constituents					
63.	*Cymbopogon citratus* (DC.) Stapf	1	Herpes simplex virus (HSV-1, HSV-2)	HSV-1 and HSV-2 titer reduction	*C. citratus* volatile oil, its nanoparticle and its hydrogel encapsulated nanoparticle showed antiviral activity on Vero cells (EC_{50}s, HSV-1: 11.59 μg/mL, 1.32 μg/mL, 0.32 μg/mL; EC_{50}s, HSV-2: 6.69 μg/mL, 1.34 μg/mL, 0.33 μg/mL) [21]
64.	*Ocimum basilicum* L.	1	Hepatitis C virus (HCV)	Plaque reduction assay	MDBK cells infected with HCV treated with camphor (**110**) and 1,8-cineole (**111**) isolated from *O. basilicum* showed significant anti-HCV activity (SI values: 13.88, 9.05) [108]

Additional references for [74], [79], [95], [100], [108], [113] are Supplementary Information: [102], [128], [69], [141], [116], [155], respectively.

[a] The plant names in this article have been checked with http://www.theplantlist.org.

[b] Stigmasterol (**77**) and stigmasta-5,22-dien-3-ol (**77**) are structurally similar.

[c] Glycyrrhizic acid (**20**) and glycyrrhizin (**20**) are similar.

Monoterpenes [3]

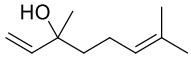

Linalool (**32**)

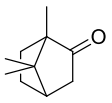

Camphor (**110**)

1,8-Cineole (**111**)

Iridoids [4]

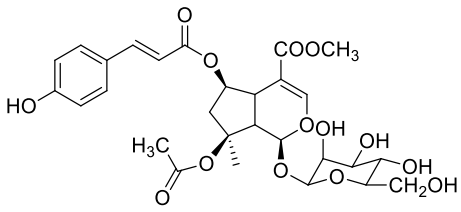

6-O-*trans*-p-Coumaroyl-8-O-acetylshanzhiside methyl ester (**7**)

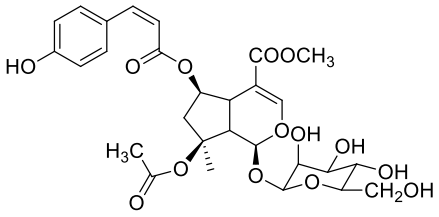

6-O-*cis*-p-Coumaroyl-8-O-acetylshanzhiside methyl ester (**8**)

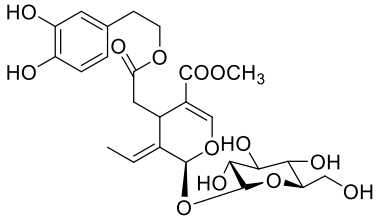

Oleuropein (**22**)

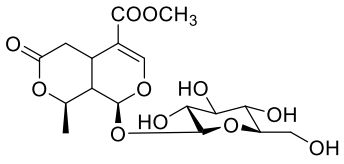

8-*epi*-Kingiside (**23**)

Sesquiterpenes [8]

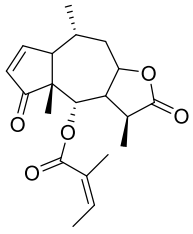

Brevilin A (**10**)

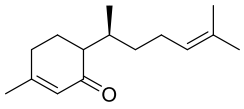

Bisabola-3,10-dien-2-one (**15**)

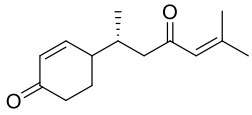

4-(6-Methyl-4-oxohept-5-en-2-yl) cyclohex-2-en-1-one (**16**)

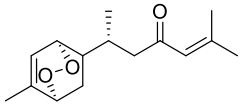

1,4-Epidioxybisabola-2,10-dien-9-one (**17**)

Fig. 1. Structures of antiviral lead molecules from medicinal plants listed for *Jwara* in *Charaka Samhita* and *Susruta Samhita*.

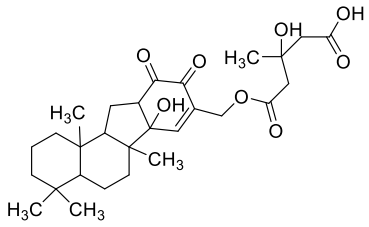

Dasyscyphin C (**18**)

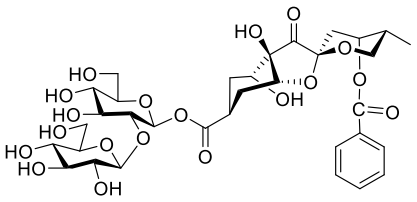

Phyllaemblicin B (**33**)

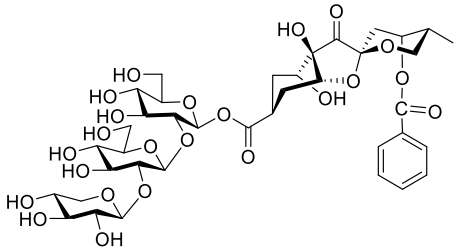

Phyllaemblicin C (**34**)

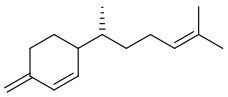

β-Sesquiphellandrene (**54**)

Diterpenes [6]

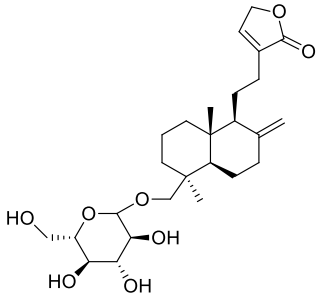

Neoandrographolide (**3**)

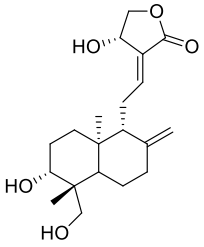

Andrographolide (**4**)

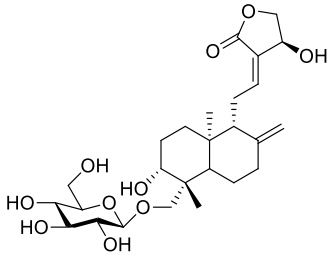

Andropanolide B (**5**)

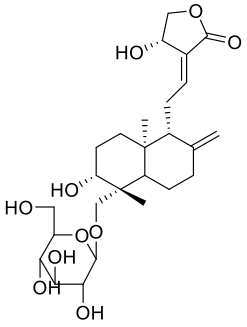

Andrographiside (**6**)

Fig. 1. (*continued*).

Rhizome hexane extract of *A. calamus* (sweet flag) displayed notable inhibition of HIV-1 reverse transcriptase activity *in vitro* (IC_{50} 32.96 μg/mL) [109]. *A. indica* (neem) seed kernel alcohol extract (fourth fraction) showed DPV inhibitory activity in CPE (cytopathic effect) inhibition assay (IC_{50} 10.9 μg/mL) [110]. Hot water extract of dried twigs of *C. cassia* (Chinese cinnamon) demonstrated significant antiviral activity against HRSV infection in HEp-2 and A549 cells, near-completely inhibiting plaque formation at 30 μg/mL (IC_{50}s 7.2 and 6.8 μg/mL, respectively) [89]. Antiviral activity of the alcoholic extract of *C. pareira* (velvet leaf) aerial parts (Cipa extract) was highest against DENV-2 and DENV-4, (IC_{50}s 1.97, 1.23 μg/mL), while against DENV-1 and DENV-3 the extract showed higher IC_{50}s (11.11 and 3.17 μg/mL, respectively); additionally, the Cipa extract was effective against a DENV-3 variant (IC_{50} 12.0 μg/mL) [90]. Sulfated derivative of pectin (SPCm) extracted from the pulp of *C. melo* (muskmelon) exhibited antiviral activity against both ACV-sensitive (KOS) and ACV-resistant (AR-29) strains of herpes simplex virus, with IC_{50}s of 6.0 and 12.0 μg/mL, respectively [104]. *C. longa* (turmeric) extract (containing 19% curcuminoid) treated on DENV-2 before infecting to the Huh7it-1 cells showed inhibition of DENV-2 concentration dependently, and 100% viral inhibition was

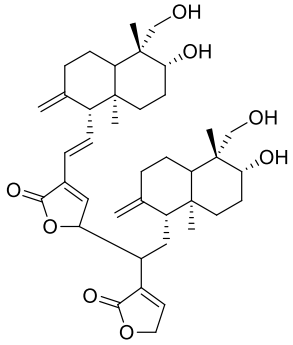

Bisandrographolide A (**60**)

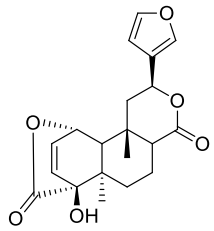

Isocolumbin (**98**)

Triterpenes [15]

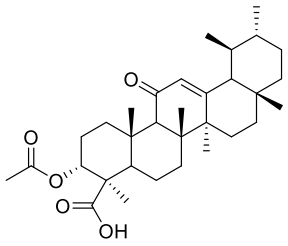

Acetyl-11-keto-β-boswellic acid (**9**)

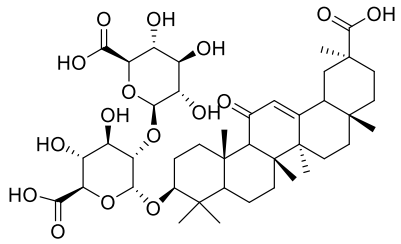

Glycyrrhizin (**20**)#

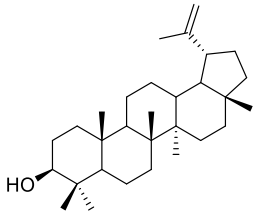

Lupeol (**21**)

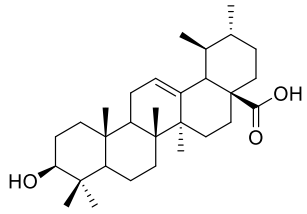

Ursolic acid (**30**)

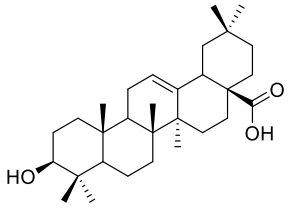

Oleanolic acid (**46**)

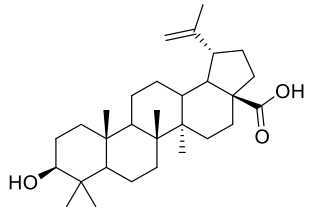

Betulinic acid (**55**)

Fig. 1. (*continued*).

observed at 80.0 μg/mL (IC_{50} 17.91 μg/mL) [93]. Ethanol extract of *C. domestica* (synonym *C. longa*) rhizomes showed significant inhibition of HCV replication on Huh 7it cells (IC_{50} 1.68 μg/mL) [94]. *C. longa* methanol extract inhibited polio virus at MNTC (maximum non-toxic concentration) of 0.03 μg/mL (IC_{50} 0.07 μg/mL) [95]. Polysaccharide rich fraction from *H. vulgare* (barley) brans showed notable inhibition of viral growth in MDCK cells (IC_{50} 23.73 μg/mL) [105]. Protein fractions of *M. pruriens* (velvet bean) seeds treated on human hepatoma cell line infected with HCV displayed anti-HCV activity in the peptide fraction of 5–10 kDa (IC_{50} 19.40 μg/mL) [107]. Ethanolic extract (100 μg/mL) of *N. nucifera* (sacred lotus) seeds, its fraction (50 μg/mL) and subfraction (50 μg/mL) displayed anti-HSV-1 activity in HeLa cells; the sub-fraction showed dose dependent anti-HSV activity (IC_{50} 21.3 μg/mL) [96]. Antioxidant macromolecular component (polysaccharide-protein complex) obtained from *N. nucifera* rhizomes inhibited RT and HIV-1 3′-processing (IC_{50}s 33.7 and 5.28 μM, respectively) [106]. *P. niruri* (gale of the wind) ethanol extract evaluated for its anti-HCV activities in Huh 7it-1 cells demonstrated strong inhibition against HCV (IC_{50} 4.14 μg/mL) [97]. *P. zeylanica* (white leadwort) 90% ethanol extract and its ZnONPs (zinc oxide nanoparticles) on treatment in Vero cells challenged with HSV-1 showed significant anti-herpetic activity (IC_{50}s 54.6 and 23.17 μg/mL, respectively) [111]. Crude ethanolic extract of *P. granatum*

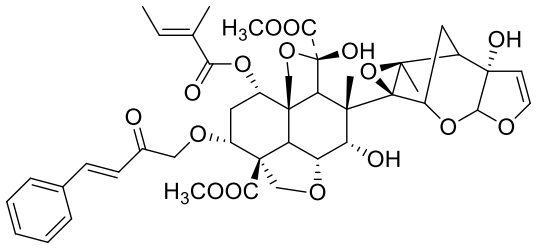

3-Deacetyl-3-cinnamoyl-azadirachtin (**64**)

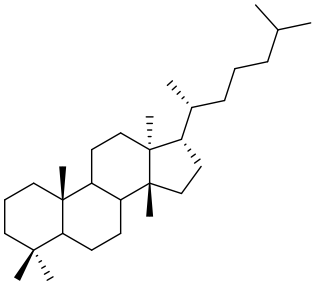

Euphane (**68**)

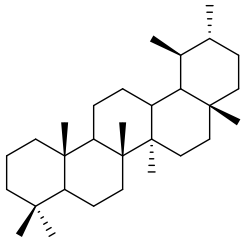

Ursane (**69**)

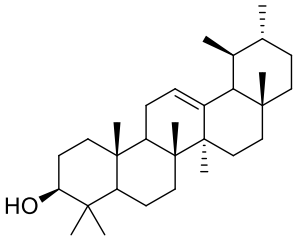

α-Amyrin (**70**)

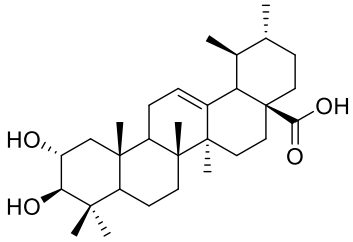

2,3-Dihydroxyurs-12-en-28-oic acid (**71**)

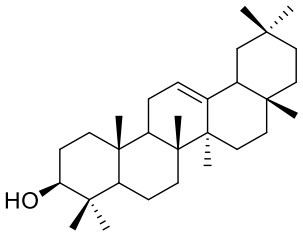

β-Amyrin (**76**)

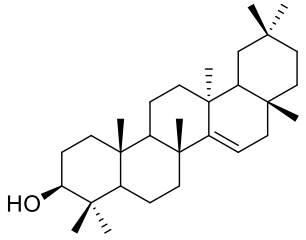

Taraxerol (**83**)

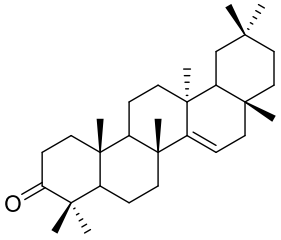

Taraxerone (**84**)

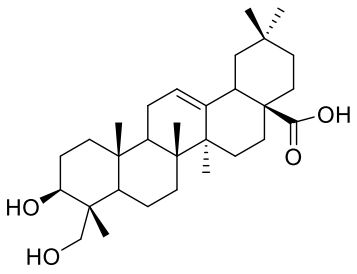

Hederagenin (**90**)

Fig. 1. (*continued*).

Steroids [13]

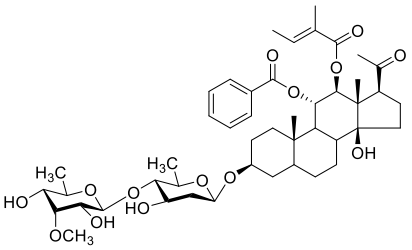

Marstenacisside D7 (**24**)

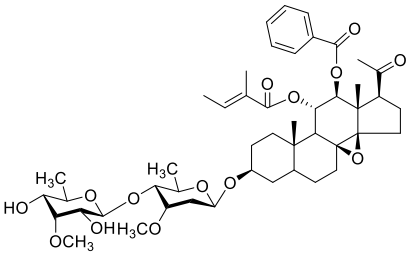

Marstenacisside E6 (**25**)

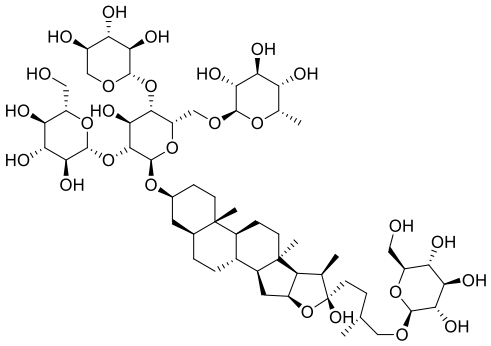

Asparoside-D (**61**)

Fig. 1. (*continued*).

(pomegranate) peel, its ethyl acetate and n-butanol fractions treated on MDCK cells infected with influenza virus A (H1N1) displayed antiviral activity with IC_{50} values of 6.45, 5.60 and 6.07 μg/mL, respectively [98]. *P. granatum* ethanol extract and its fraction containing punicalagin (**37**, ellagitannin) treated with Vero cells infected with Mayaro virus displayed antiviral activities with IC_{50}s 12.3 and 29.9 μg/mL, respectively [99]. Ethanol extract of *P. granatum* dried peels treated on HeLa cells infected with adenovirus (type 5) showed complete inhibition of the CPE at 30.0 μg/mL (IC_{50} 18.6 μg/mL) [100]. Again, the ethanol extract of *P. granatum* shell and punicalagin (**37**) treated on Vero cells infected with MAYV displayed significant activity with IC_{50} values of 12.3 and 28.2 μg/mL, respectively [101]. HIV-$1_{NL4.3,}$ when pretreated with aqueous and 50% ethanolic extracts of *R. parviflora* (small flowered poison sumac) leaves mixed with TZM-bl, showed dose dependent inhibition in HIV-1 infection (IC_{50}s 15.0 and 26.0 μg/mL, respectively); in CEM-GFP assay, IC_{50} values of the aqueous and 50% ethanolic extracts were 65.0 and 29.0 μg/mL, respectively [112]. *S. indicus* (East Indian globe thistle) leaf aqueous extract treated on infected MT-4 cells showed inhibition of HIV-1 replication with an IC_{50} of 52.35 μg/mL [113]. Ethanolic extract (50%) of *T. chebula* (chebulic myrobalan) fruits, chebulagic acid (**47**) (benzopyran tannin) and chebulinic acid (**48**) (ellagitannin) showed direct HSV-2 inhibitory activity on Vero cells (IC_{50}s 0.01, 1.41, 0.06 μg/mL); the extract and the two compounds inhibited the binding of HSV-2 to Vero cells dose-dependently with very low IC_{50} values of 0.48, 1.66, and 0.29 μg/mL, respectively [51]. Methanolic extract of *T. populneoides* (Indian tulip tree) flowers displayed strong activity on HeLa cells infected with vesicular stomatitis, coxsackie and respiratory syncytical viruses with EC_{50} values of 20.0 μg/mL [102].

The oxygenated monoterpene, linalool (**32**) (*O. basilicum*, basil), showed strongest activity against AVD-II (BCC-1/KMC cells, EC_{50} 16.9 μg/mL) [42]. Brevilin A (**10**) (sesquiterpene lactone, *C. minima*, spreading sneezeweed) showed strong anti-influenza activity against various strains of viruses, including PR8, H1N1 (FM1), H3N2, and H9N2, with very low EC_{50}s 2.96, 1.60, 3.28, and 2.07 μM, respectively [30]. Tatanan A (**1**, sesquilignan, *A. calamus*, sweet flag) demonstrated anti-DENV activity with a low EC_{50} of 3.9 μM [22]. Ursolic acid (**30**) (triterpenoid, *O. basilicum*) showed strongest activities against HSV-1 (EC_{50} 6.6 μg/mL), ADV-8 (EC_{50} 4.2 μg/mL), CVB1 (EC_{50} 0.4 μg/mL) and EV71 (EC_{50} 0.5 μg/mL) [42]. Two iridoid glycosides, 6-*O*-*trans*--*p*-coumaroyl-8-*O*-acetylshanzhiside methyl ester (**7**) and 6-*O*-*cis*-*p*-coumaroyl-8-*O*-acetylshanzhiside methyl ester (**8**), from *B. prionitis*

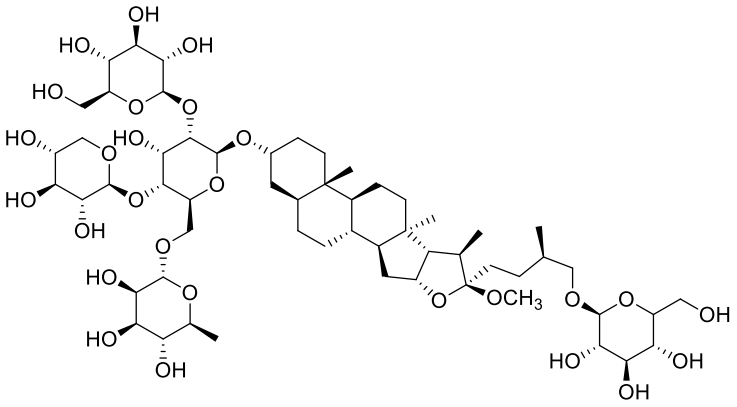

Asparoside-C (**62**)

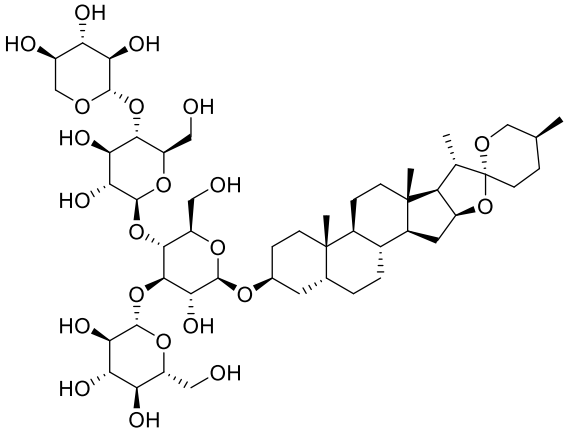

Asparoside-F (**63**)

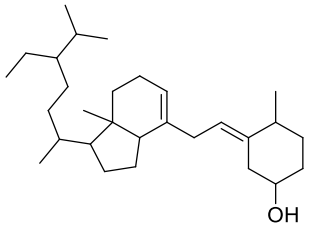

Boerhavisterol (**67**)

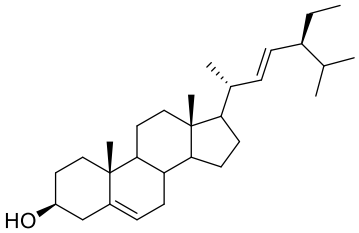

Stigmasterol (**77**)*

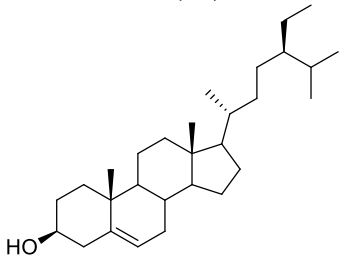

β-Sitosterol (**102**)

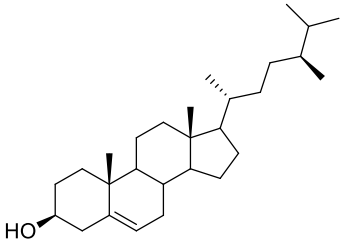

Campesterol (**103**)

Fig. 1. (*continued*).

(porcupine flower) at 3:1 combination displayed significant anti-RSV activity (EC_{50} 2.46 μg/mL) [27]. Three bisbenzylisoquinoline alkaloids, liensinine (**26**), neferine (**27**) and isoliensinine (**28**) (*N. nucifera*, sacred lotus), showed strong anti-HIV-1 activity with EC_{50}s of <0.8 μg/mL, and nuciferine (**29**) (aporphine alkaloid, *N. nucifera*) displayed anti-HIV activity with EC_{50} 0.8 μg/mL [41]. Cyclopeptide alkaloids, jubanine H (**56**) and nummularine B (**57**), isolated from the methanol extract of *Z. jujuba* (Indian jujube, Indian plum) roots displayed inhibition of PEDV in Vero cells with EC_{50} values of 4.49 and 6.17 μM, respectively [56]. Apigenin (**31**) (flavonoid, *O. basilicum*) showed high

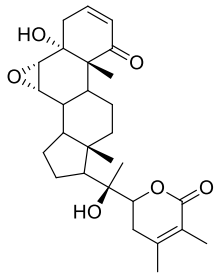

Withanolide A (**105**)

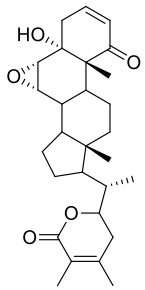

Withanolide B (**106**)

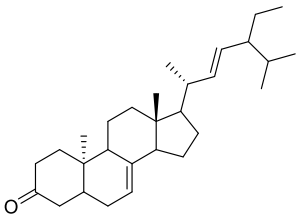

Spinasterone (**108**)

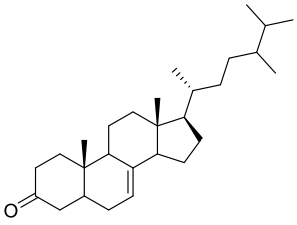

24-Methylcholesta-7-en-3β-on (**109**)

Alkaloids [13]

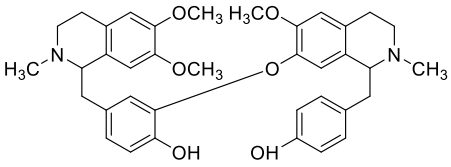

Liensinine (**26**)

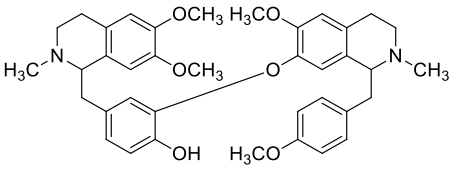

Neferine (**27**)

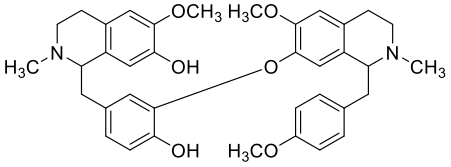

Isoliensinine (**28**)

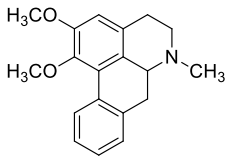

Nuciferine (**29**)

Fig. 1. (*continued*).

activity against HSV-2 (EC_{50} 9.7 μg/mL), ADV-3 (EC_{50} 11.1 μg/mL), hepatitis B surface antigen (EC_{50} 7.1 μg/mL) and hepatitis B e antigen (EC_{50} 12.8 μg/mL) [42]. Polyphenol, ellagic acid (**41**) (*P. granatum*, pomegranate), in plaque reduction assays on Vero cells infected with ZIKV-MR766 and HPF2013 strains displayed strong anti-ZIKV activity (EC_{50}s 0.86 μM) [19]. Alstotides (As1 and As3; cystine knot-amylase inhibitors) from *A. scholaris* (Indian devil tree) showed EC_{50}s 35.0 and 55.0 μM, respectively, against infectious bronchitis virus; As1 also showed moderate inhibition of DENV2 (EC_{50} 90.0 μM) [114].

The sesquiterpene, β-sesquiphellandrene (**54**) (*Z. officinale*, ginger), displayed strong activity on HeLa cells infected with rhinovirus IB (IC_{50} 0.44 μM) [54]. Bisabolane-type sesquiterpenoids *viz.*, bisabola-3, 10-dien-2-one (**15**), 4-(6-methyl-4-oxohept-5-en-2-yl)cyclohex-2-en-1-one (**16**) and 1,4-epidioxybisabola-2,10-dien-9-one (**17**) (*C. longa*, turmeric), showed significant inhibition of influenza virus-A/PR/8/34 (H1N1) replication in MDCK cells with IC_{50}s of 23.10, 11.43, and 16.79 μg/mL, respectively; bisabola-3,10-dien-2-one (**15**) also showed strong anti-H1N1 activity in A549 cells (IC_{50} 47.65 μg/mL) [33]. Drimane sesquiterpene, dasyscyphin C (**18**), from *E. prostrata* (false daisy) demonstrated viral inhibition concentration dependently (IC_{50} 20.0 μg/mL) on nodavirus infected SIGE cells [34]. Brevilin A (**10**) has displayed potent anti-influenza activity against the PR8 strain (IC_{50} 1.8 μM) [29]. The diterpene, neoandrographolide (**3**, *A. paniculata*, green chireta), showed strong anti-herpes activity (IC_{50} 7.97 μg/mL) [24]. SARS-CoV-2 infected Calu-3 cells treated with *A. paniculata* extract and andrographolide (**4**, diterpene) displayed significant plaque reduction

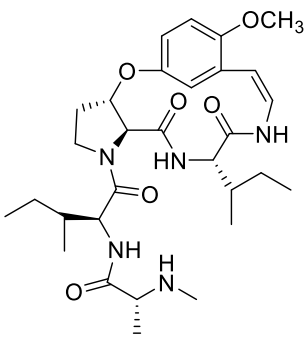

Jubanine H (**56**)

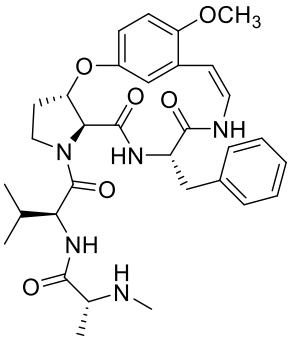

Nummularine B (**57**)

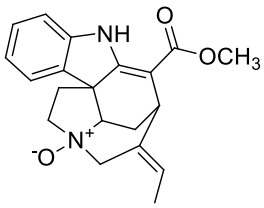

Akuammicine N-oxide (**59**)

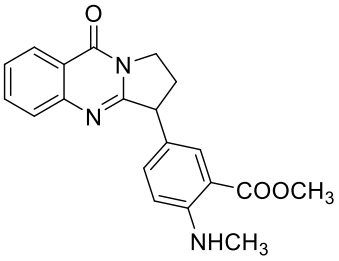

Anisotine (**79**)

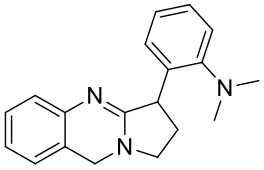

Vasicoline (**80**)

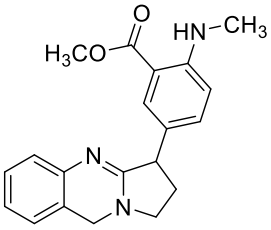

Adhatodine (**81**)

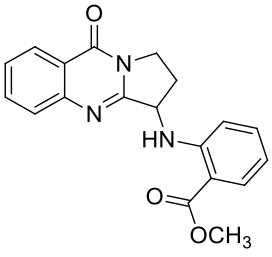

Vasnetine (**82**)

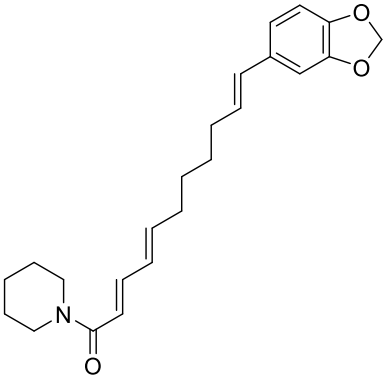

Piperundecalidine (**96**)

Fig. 1. (*continued*).

(IC_{50}s 0.036 μg/mL and 0.034 μM, respectively) [25]. Again diterpenes, andropanolide B (**5**) and andrographiside (**6**) (*A. paniculata*), showed anti-RSV effects with IC_{50} values of 25.0 and 30.0 μg/mL, respectively [26]. Norsesquiterpenoid glycosides, phyllaemblicin B (**33**) and phyllaemblicin C (**34**) (*P. emblica*, amla), exhibited strong anti-CVB3 activity with IC_{50}s 7.8 and 11.0 μg/mL, respectively [43].

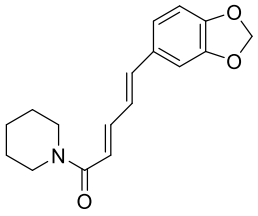

Piperine (**97**)

Flavonoids [21]

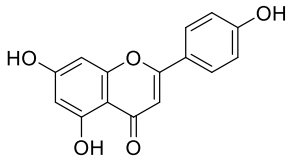

Apigenin (**31**)

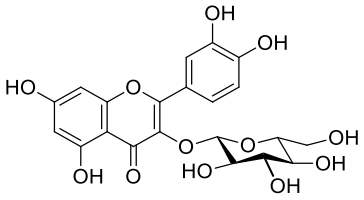

Isoquercetin (**38**)

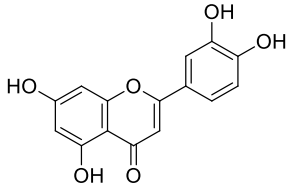

Luteolin (**39**)

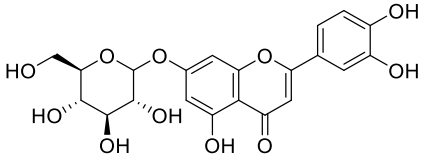

Luteolin-7-O-glucoside (**42**)

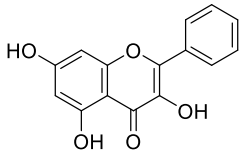

Galangin (**58**)

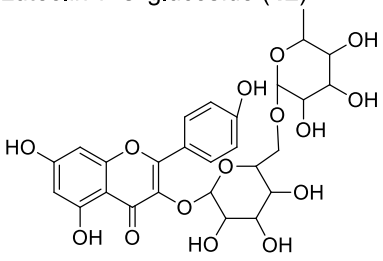

Biorobin (**65**)

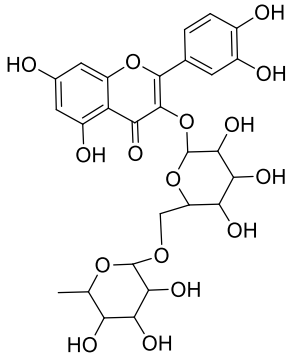

Bioquercetin (**66**)

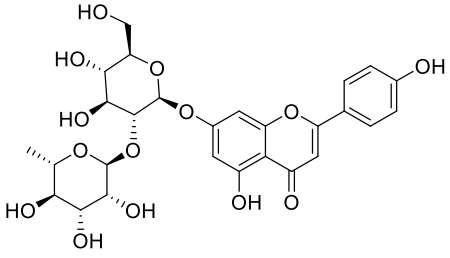

Rhoifolin (**72**)

Fig. 1. (*continued*).

Acetyl-11-keto-β-boswellic acid (**9**) (triterpene, gum resin extract of *B. serrata*, Indian frankincense) inhibited transduction of cells with CHIKV-E2/E1 and VSV-G pseudotyped vectors with IC_{50} values of 6.75 and 5.97 μM, respectively [28]. 293T cells infected with CHIKV-luci or VSV-luci in presence of acetyl-11-keto-β-boswellic acid (**9**) (*B. serrata*) showed significant decrease in viral infection (IC_{50}s 4.51 and 2.30 μM, respectively) [28]. Lupeol (**21**) (pentacyclic triterpene) and the root powder decoction (*H. indicus*, Indian sarsaparilla) demonstrated strong activity against HIV–I RT RNase H with IC_{50}s of 11.6 and 2.9 μM, respectively [37]. Flavonol, quercetin (**89**), from *M. dioica* (spiny gourd)

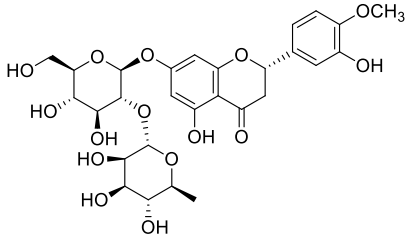

Neohesperidin (**73**)

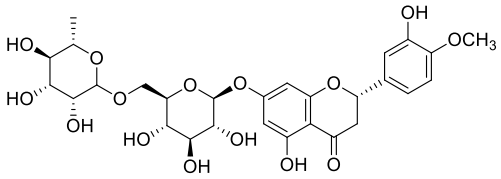

Hesperidin (**74**)

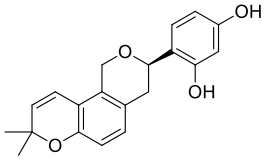

Glabridin (**78**)

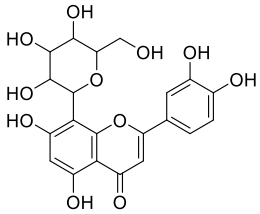

Orientin (**86**)

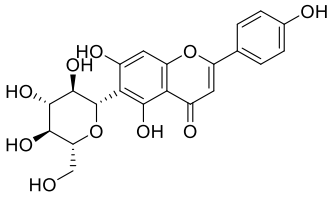

Isovitexin (**87**)

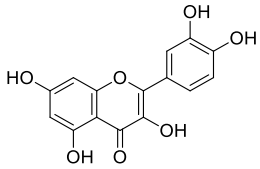

Quercetin (**89**)

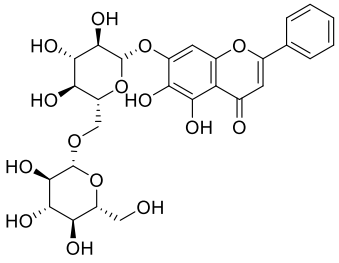

Baicalein-7-O-diglucoside (**91**)

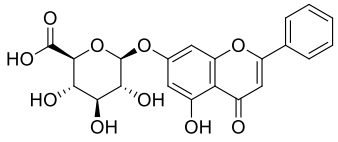

Chrysin-7-O-glucuronide (**92**)

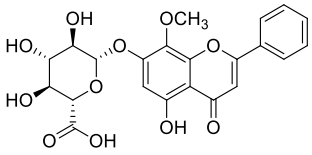

Oroxindin (**93**)

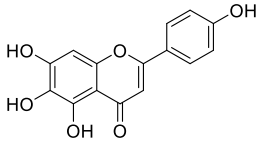

Scutellarein (**94**)

Fig. 1. (*continued*).

displayed highest inhibition of SARS-CoV-2 main protease (IC_{50} 0.06 μM) and spike protein (IC_{50} 0.05 μM), and the polyphenol, catechin (**88**) (*M. dioica*), showed highest inhibition of RdRp (IC_{50} 0.71 μM) and DPP4 protein (IC_{50} 0.03 μM) [76]. Glycyrrhizin (**20**) (triterpene, *G. glabra*, licorice or sweetwood) displayed dose-dependent antiviral activity in Huh-7 cells infected with HCV; RT-PCR analysis showed 50% reduction in HCV at 14.0 μg [36]. Beta-diketone derivatives, demethoxy curcumin (**12**), bisdemethoxy curcumin (**13**) and curcumin (**11**) (*C. longa*, turmeric), exhibited strong inhibitory activity against the neuraminidases from novel influenza H1N1 (WT) (IC_{50}s 4.36, 6.95, 3.46 μg/mL); 1,5-bis(4-hydroxyphenyl)-1,4-pentadiene-3-one (**14**) (phenolic compound, *C. longa*) showed IC_{50}s of 6.18 and 3.77 μg/mL against influenza A H1N1 and H9N2, and curcumin (**11**) displayed IC_{50} of 6.17 μg/mL against influenza A H9N2 strain expressed in 293T cells [31]. Curcumin (**11**) and its derivatives, gallium-curcumin and cu-curcumin (*C. longa*), on testing their effects on replication of HSV-1 in Vero cells displayed notable antiviral activity with IC_{50} values of 33.0, 13.9, and 23.1 μg/mL, respectively [32]. Garcinol (**19**) (polyisoprenylated benzophenone derivative, *G. indica*, kokum) showed strong inhibition of wild-type HIV-1-RNase H (IC_{50} 6.6 μM) [35]. HBsAg secretion from HBV transfected HepG2 2.2.15 cells was inhibited by the secoiridoid glycoside, oleuropein (**22**) (*J. grandiflorum*, jasmine), dose-dependently (IC_{50} 23.2 μg/mL) [38]. HBV transfected HepG2 2.2.15 cells treated with 8-*epi*-kingiside (**23**) (secoiridoid glycoside, *J. grandiflorum*) displayed

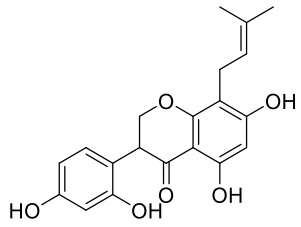

Kievitone (**99**)

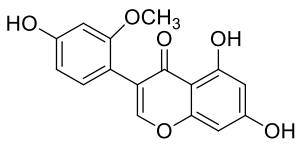

Isoferreirin (**101**)

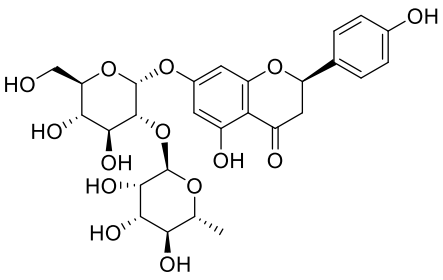

Naringin (**104**)

Phenolics [13]

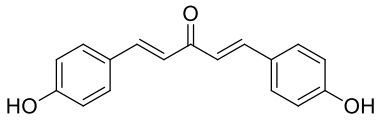

1,5-Bis(4-hydroxyphenyl)-1,4-pentadiene-3-one (**14**)

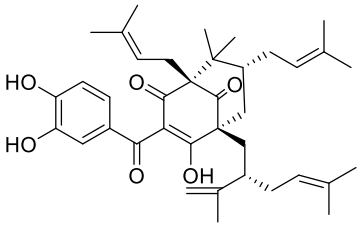

Garcinol (**19**)

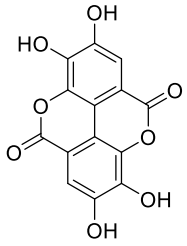

Ellagic acid (**41**)

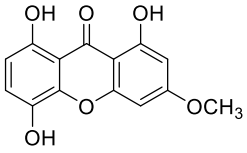

Bellidifolin (**45**)

Fig. 1. (*continued*).

significant reduction of HBsAg secretion dose-dependently (IC_{50} 19.4 μg/mL) [39]. Again, treatment of HepG2.2.15 cells with the dibenzylbutane lignin, niranthin (**35**) (*P. niruri*, gale of the wind), at various concentrations for 4 days resulted in dose-dependent reduction of HBsAg and HBeAg secretion, with IC_{50}s of 15.6 and 25.1 μM, respectively [44]. Punicalagin (**37**), punicalin (**40**) (ellagitannins, *P. granatum*, pomegranate) and ellagic acid (**41**) displayed strong inhibition of HIV-1 RT-associated RNase H function (IC_{50}s 0.12, 0.18 and 1.4 μM, respectively) and HIV-1 integrase LEDGF-dependent activities (IC_{50}s 0.07, 0.09 and 0.08 μM, respectively); luteolin (**39**) and apigenin (**31**) (flavonoids, *P. granatum*) showed inhibition of RNase H and IN functions with IC_{50} values of 3.7–22.0 μM [48]. Casuarinin (**49**) (ellagitannin, *T. chebula*, chebulic myrobalan), pentagalloyl glucose (**50**) (polyphenol, *T. chebula*) and chebulagic acid (**47**) (*T. chebula*) demonstrated significant HCV protease inhibitory activity with IC_{50} values of 9.6, 10.6 and 5.2 μM, respectively [52]. Naphthohydroquinones, furomollugin (**43**) and mollugin (**44**) (*R. cordifolia*, Indian madder), treated on Hep3B cells inhibited the secretion of hepatitis B surface antigen, with IC_{50} values of

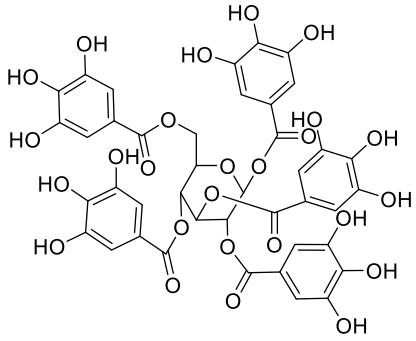

Pentagalloyl glucose (**50**)

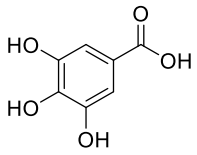

Gallic acid (**51**)

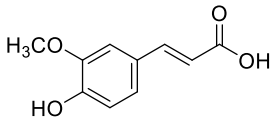

Ferulic acid (**85**)

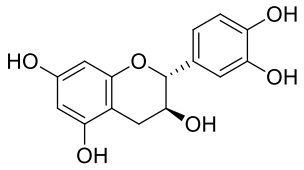

Catechin (**88**)

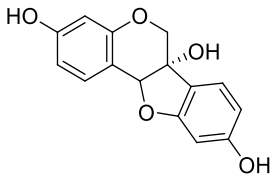

Glycinol (**100**)

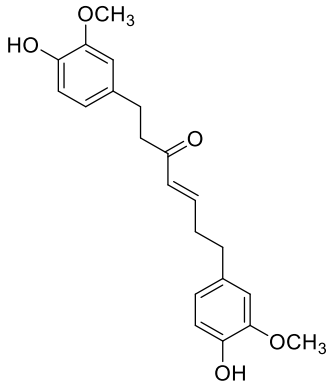

Gingeronone A (**107**)

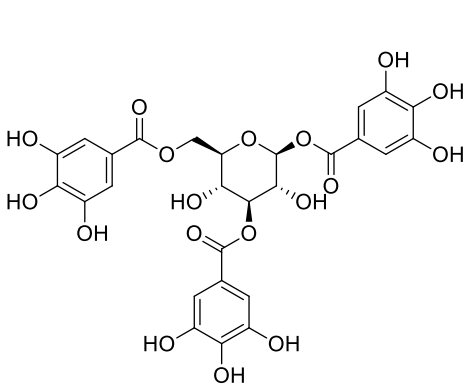

1,3,6-Tri-O-galloyl-β-D-glucopyranose (**52**)

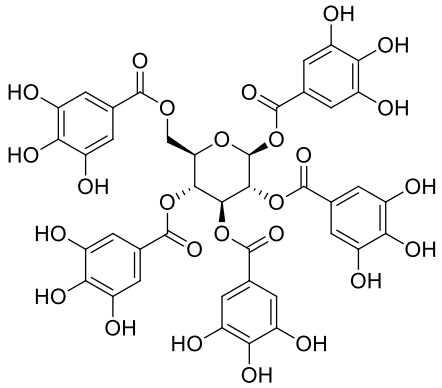

1,2,3,4,6-Penta-O-galloyl-β-D-glucopyranose (**53**)

Fig. 1. (*continued*).

2.0 μg/mL [49]. Two galloyl glucoses, (1,3,6-tri-*O*-galloyl-β-D-glucopyranose (**52**), 1,2,3,4,6-penta-*O*-galloyl-β-D-glucopyranose (**53**)), and chebulagic acid (**47**)), showed very good inhibitory activities against 3′-processing of HIV-1 integrase (IC_{50}s 13.7–19.7 μM), while against reverse transcriptase, chebulagic acid (**47**) only showed significant inhibitory action (IC_{50} 20.6 μM) [53].

Hydroalcoholic extract of *C. pareira* (velvet leaf) whole plant showed 98% inhibition against SARS-CoV-2 *in vitro* [115]. Methanol extract (80%) of *A. maurorum* (camel thorn) aerial parts displayed potent CPE at 3.0 μg/mL in FMDV infected RBK cells [87]. Anti-CHIKV ethanolic

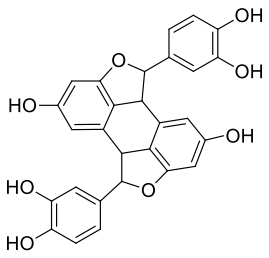

Jezonofol (**75**)

Phenylpropanoid [1]

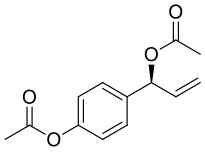

1'-S-1'-Acetoxychavicol acetate (**2**)

Naphthoquinones [2]

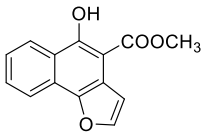

Furomollugin (**43**)

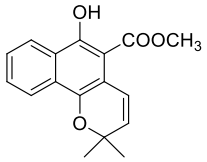

Mollugin (**44**)

Diarylheptanoids [3]

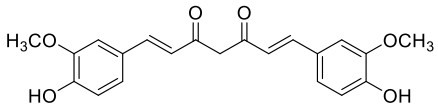

Curcumin (**11**)

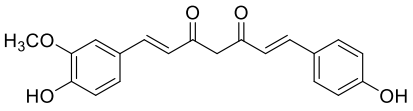

Demethoxy curcumin (**12**)

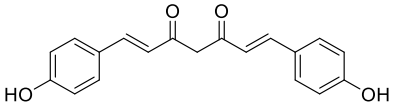

Bisdemethoxy curcumin (**13**)

Fig. 1. (*continued*).

fraction of *C. dactylon* (Bermuda grass) at 50 μg/mL exhibited viral inhibitory activity (about 98%) by reduction in cytopathic effect [116]. *C. dactylon* ethanolic extract (20% extract, in the feed) showed highest protective activity of 91.1% against IMNV in *Penaeus vannamei* Boone *(Litopenaeus vannamei* Boone) [117]. Dichloromethane (25-10 μg/mL) and 25% ethanol (50-25 μg/mL) extracts of *H. pubescens* (Indrajao) stem bark displayed significant plaque reduction (90%) in HeLa Ohio cells infected with rhino virus type 2 [118]. Aqueous, ethanolic and aqueous-ethanolic extracts of *P. granatum* (pomegranate) leaves showed significant anti-HHV3 activity on cultured HEp-2 cells; MIC values of aqueous extract on HHV-3 from Chickenpox and Herpes Zoster were 15.62 and 31.25 μg/mL, respectively [47]. *T. ammi* (ajowan) seed essential oil on pre-exposure to JEV showed 80% virus inhibition at 0.5 mg/mL in Vero cells [119].

Betulinic acid (**55**, pentacyclic triterpenoid) isolated from *Z. jujuba* (Indian plum) roots, at 10 and 50 μM concentrations, treated on A549 human lung adenocarcinoma epithelial cells infected with A/PR/8/34 virus displayed 30% and 98% inhibition, respectively [55]. In luciferase assay, steroidal glycosides, marstenacisside D7 (**24**) and marstenacisside E6 (**25**) (*M. tenacissima*, devil's tongue), displayed 81.3 and 80.9% inhibition of HIV-1, respectively [40]. Phenylpropanoid, 1′S-1′-acetoxychavicol acetate (**2**) (*A. galangal*, galangal), at 4 μM

Tannins [5]

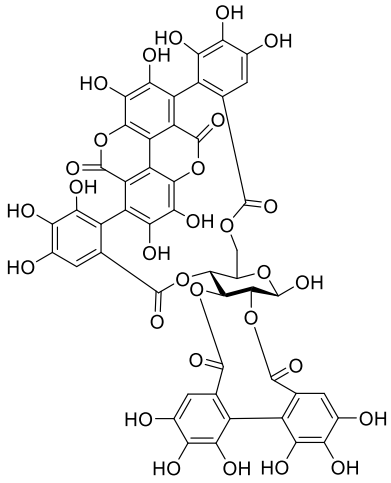

Punicalagin (**37**)

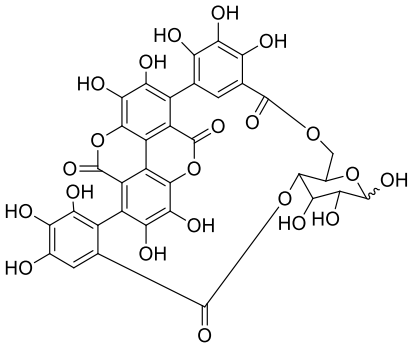

Punicalin (**40**)

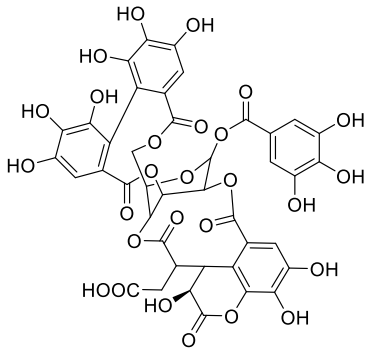

Chebulagic acid (**47**)

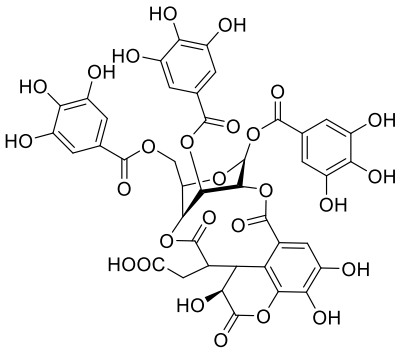

Chebulinic acid (**48**)

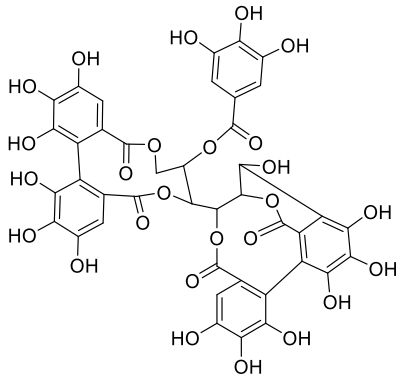

Casuarinin (**49**)

Fig. 1. (*continued*).

completely inhibited the export of RevNES fusion protein from HIV-1 nucleus [23]. Punicalagin (**37**) isolated from the fruit peel ethanolic extract of *P. granatum* at 31.25 μg/mL displayed 100% anti-HSV-2 activity, comparable to that of standard drug acyclovir [46].

Several reports in Table 1 and Table S3 are describing molecular docking analysis on the inhibitory effects of secondary metabolites (ligands) of the plants listed in '*Charaka Samhita*' and '*Sushruta Samhita*' for '*Jwara*' on various viral targets (examples: Utomo et al., 2020; Shah et al., 2021; Ram et al., 2022) [57,58,77]. A handful of studies, prompted by the recent global outbreak, are also on SARS-CoV-2 virus (examples: Banerjee et al., 2021; Murugan et al., 2021; Sa-Ngiamsuntorn et al., 2021; Nedungadi et al., 2023; Patwardhan, 2023) [9,10,25,59,120].

Phytochemicals in these lead plants showed varying levels of activities against a wide spectrum of pathogenic viruses. The structural groups of individual molecules of these medicinal plants with most significant antiviral activities (low EC_{50}/IC_{50}/LC_{50}, high % inhibition) are flavonoids (21), triterpenes (15), alkaloids (13), phenolics (13), steroids (13), sesquiterpenes (8), diterpenes (6), tannins (5), iridoids (4), lignans (4), diarylheptanoids (3), monoterpenes (3), naphthoquinones (2), and phenylpropanoid (1) (Table 1, Fig. 1). Similarly, the most promising individual compounds obtained are tatanan A (**1**), 1′S-1′-acetoxychavicol acetate (**2**), neoandrographolide (**3**), andrographolide (**4**), andropanolide B (**5**), andrographiside (**6**), 6-*O*-*trans*-*p*-coumaroyl-8-

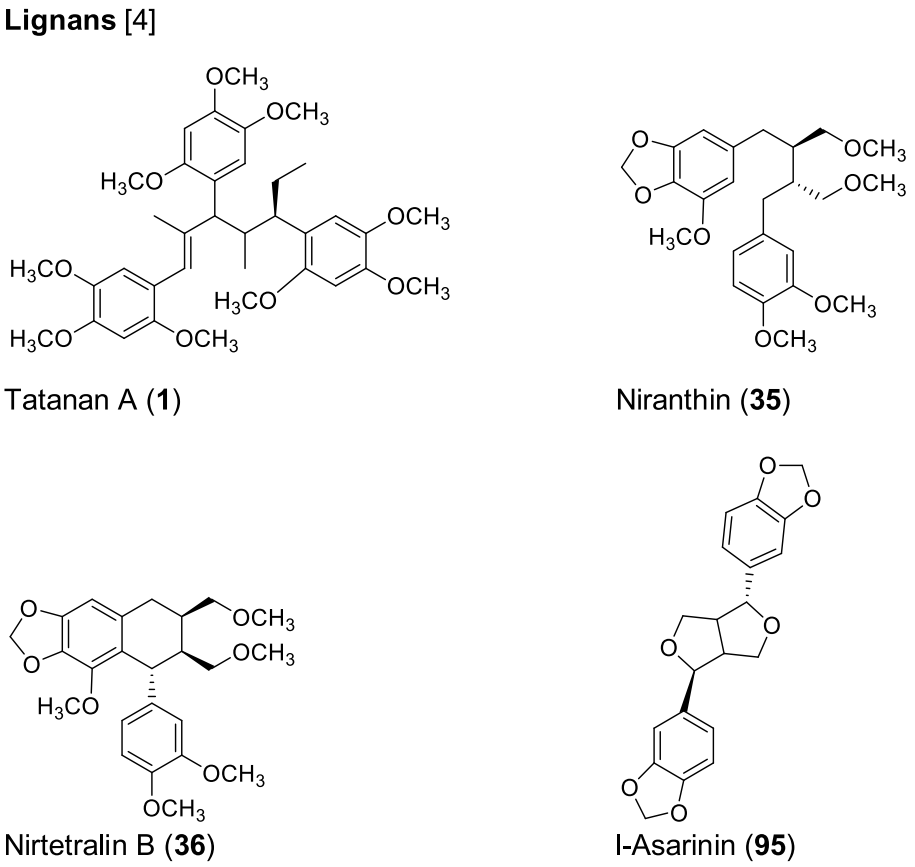

Fig. 1. (*continued*).

O-acetylshanzhiside methyl ester (**7**), 6-*O*-cis-*p*-coumaroyl-8-*O*-acetyl-shanzhiside methyl ester (**8**), acetyl-11-keto-β-boswellic acid (**9**), brevilin A (**10**), curcumin (**11**), demethoxy curcumin (**12**), bisdemethoxy curcumin (**13**), bisabola-3,10-dien-2-one (**15**), 4-(6-methyl-4-oxohept-5-en-2-yl)cyclohex-2-en-1-one (**16**), 1,4-epidioxybisabola-2,10-dien-9-one (**17**), dasyscyphin C (**18**), glycyrrhizin (**20**), lupeol (**21**), oleuropein (**22**), 8-*epi*-kingiside (**23**), marstenacisside D7 (**24**), marstenacisside E6 (**25**), liensinine (**26**), neferine (**27**), isoliensinine (**28**), ursolic acid (**30**), apigenin (**31**), linalool (**32**), phyllaemblicin B (**33**), phyllaemblicin C (**34**), niranthin (**35**), punicalagin (**37**), luteolin (**39**), punicalin (**40**), ellagic acid (**41**), furomollugin (**43**), mollugin (**44**), chebulagic acid (**47**), chebulinic acid (**48**), casuarinin (**49**), pentagalloyl glucose (**50**), 1,3,6-tri-*O*-galloyl-β-D-glucopyranose (**52**), 1,2,3,4,6-penta-*O*-galloyl-β-D-glucopyranose (**53**), β-sesquiphellandrene (**54**), betulinic acid (**55**), jubanine H (**56**), nummularine B (**57**), catechin (**88**), and quercetin (**89**) (Fig. 1). The structures of these molecular entities are compatible in displaying antiviral activities due to their substitutions and functional groups. Compounds with more number of hydroxyl groups displayed higher antiviral activity. Methoxy substituted entities showed less antiviral activity than the ones with methyl groups. The relative position of functional groups is also a factor deciding the antiviral efficacy of these lead molecules. Aromatic phytochemicals (phenolic compounds) with methoxy group at second or sixth position displayed higher antiviral activity than compounds with methoxy substitution at third or fourth position of the aromatic ring [121,122]. In addition, modifications of the OH- or –COOH functional groups of phytochemicals also resulted in enhancement of their antiviral activities [123].

In these antiviral studies (Table 1), very low $EC_{50}/IC_{50}/LC_{50}$ and high percentage inhibitions were demonstrated by the active extracts and constituents of the medicinal plants, *A. calamus*, *A. galanga*, *A. indica*, *A. lanata*, *A. maurorum*, *A. paniculata*, *A. scholaris*, *B. prionitis*, *B. serrata*, *C. cassia*, *C. citratus*, *C. dactylon*, *C. longa*, *C. melo*, *C. minima*, *C. pareira*, *E. prostrata*, *G. glabra*, *G. indica*, *H. indicus*, *H. pubescens*, *H. vulgare*, *J. adhatoda*, *J. grandiflorum*, *M. dioica*, *M. pruriens*, *M. tenacissima*, *N. alba*, *N. nucifera*, *O. basilicum*, *O. sanctum*, *P. emblica*, *P. granatum*, *P. niruri*, *P. roxburghii*, *P. zeylanica*, *R. cordifolia*, *R. parviflora*, *S. indicus*, *T. ammi*, *T. chebula*, *T. populneoides*, *Z. jujuba*, and *Z. officinale*. These plants are widely used as traditional medicines, vegetables, food and flavours for over centuries.

6. Natural products, antiviral drug development

Viral diseases are consistent threats to human life on Earth, and they cause considerable burden on public health and finance [124]. The World Health Organization (WHO) and the United Nations (UN) have emphasized the specific need for better management of viral diseases [125]. The COVID-19 pandemic has further highlighted the importance of new generation antiviral drugs, and in 2022 the National Institute of Allergy and Infectious Diseases (NIAID), a wing of the National Institutes of Health (NIH), has awarded approx. $ 577 million to set up nine Antiviral Drug Discovery (AViDD) Centers for Pathogens of Pandemic Concern [126]. The development of novel antiviral drugs is arduous and often unprofitable; the current strategy for the management of viral outbreaks is mostly through vaccines over antiviral treatments. Antiviral drugs are approved medicines that prevent virus multiplication. Now, there are 179 approved antiviral drugs derived from 88 unique structural entities. Moreover, thousands of antiviral agents are in preclinical and hundreds in clinical trials. It takes nearly 15 years and 2 billion USD to develop a new drug from an antiviral agent [124]. Antiviral drugs also display aftereffects such as drowsiness, nausea, vomiting, allergic reactions, insomnia, heart problems, and dependence; and many of them have been withdrawn due to these side effects [124].

Viral structure and replication are crucial factors deciding the design

of antiviral drugs. Nature has provided yet another source of antiviral agents, and almost 40% of the drugs available at the moment are directly or indirectly plant derivatives. Herbal remedies and extracted natural products often provide a significant source of unique antiviral drugs [127,128]. Plant based secondary metabolites (flavonoids, alkaloids, terpenoids, steroids, phenolics, iridoids, essential oils), anthocyanins, polyphenols, short peptides and polysaccharides have the capability to interfere with membrane permeability, cellular functions and replication cycle of viruses [127,129]. The antiviral activity of plant secondary metabolites and other active entities are determined through various assays such as cytotoxicity, cytopathic effect, and the capability to block viral spread between cells. The mechanistic approaches described in Table 1 and Table S3 are primarily based on the interference of viral entry and prevention of their replication. Medicinal plants listed for the treatment of '*Jwara*' in '*Charaka Samhita*' and '*Sushruta Samhita*' are time tested and with proven effects in traditional practices. This review demonstrates that plants listed for fever in the ancient wisdom of *Ayurveda* and their molecular entities could serve as a repository for the design of antiviral agents [9].

7. Conclusions and future perspectives

Ayurveda and other traditional systems use an array of medicinal plants, and recently with the advances in phytochemistry, metabolomics and pharmacology, the molecular entities causing their medicinal effects and their mechanisms are being elucidated. Systematic studies on plants listed in the *Samhitas* of *Charaka* and *Sushruta* for treatment of '*Jwara*' (fever) have resulted in promising leads against several viruses. Strikingly, of the 250 medicinal plants listed in these two earliest Ayurvedic treatises, only 80 were subjected to antiviral studies so far. Among these, the plants demonstrated excellent antiviral activities are widely used as foods, flavours, vegetables and in traditional medicines. This review is providing systematic mechanistic studies as evidences towards the traditional antiviral claims on these medicinal plants.

Secondary metabolites (including essential oils), anthocyanins, polyphenols, short peptides and polysaccharides of these medicinal plants are interfering cellular functions and replication cycles of viruses. These structural entities offer options of deriving their synthetic analogues and assessing their antiviral potentials. The promising molecular entities could be chosen for further investigations towards the development of antiviral agents. Moreover, this review emphasizes the need of antiviral studies on hitherto uninvestigated plants listed for the treatment of '*Jwara*' in these two *Samhitas*.

Author contributions

AB: Literature survey, data curation, formal analysis, validation, writing - review and editing. ANS: data curation, formal analysis, validation, writing - review and editing. AJJ: data curation, formal analysis, validation, funding acquisition, writing - review and editing. SB: conceptualization, formal analysis, validation, writing - original draft, writing - review and editing. All authors approved the final version.

Declaration of generative AI in scientific writing

The authors have not used any AI tools for writing this manuscript

Funding source

This work was supported by the Kerala State Council for Science Technology and Environment, Government of Kerela (grant number Plan Project: KSCSTE/JNTBGRI P 17).

Conflict of interest

The authors declare that they have no known competing financial interests or personal relationships that could have appeared to influence the work reported in this paper.

Appendix A. Supplementary data

Supplementary data to this article can be found online at https://doi.org/10.1016/j.jaim.2024.101085.

References

[1] Rajbhandari M, Mentel R, Jha PK, Chaudhary RP, Bhattarai S, Gewali N, et al. Antiviral activity of some plants used in Nepalese traditional medicine. Evid Based Complement Altern Med 2009;6:328279. https://doi.org/10.1093/ecam/nem156.
[2] Chang JS, Wang KC, Yeh CF, Shieh DE, Chiang LC. Fresh ginger (*Zingiber officinale*) has anti-viral activity against human respiratory syncytial virus in human respiratory tract cell lines. J Ethnopharmacol 2013;145:146–51. https://doi.org/10.1016/j.jep.2012.10.043.
[3] Cock IE, Van Vuuren SF. The traditional use of southern African medicinal plants in the treatment of viral respiratory diseases: a review of the ethnobotany and scientific evaluations. J Ethnopharmacol 2020;262:113194. https://doi.org/10.1016/j.jep.2020.113194.
[4] Patwardhan B, Vaidya ADB, Chorghade M. Ayurveda and natural products drug discovery. Curr Sci 2004;86:789–99.
[5] Thomas V, Nair SNV, Ved DK, Shankar D. Controversial identities of medicinal plants in classical literature of Ayurveda. J Ayurveda Integr Med 2020;11:565–72. https://doi.org/10.1016/j.jaim.2019.09.003.
[6] Dev S. Ancient-modern concordance in Ayurvedic plants: some examples. Environ Health Perspect 1999;107:783–9. https://doi.org/10.1289/ehp.99107783.
[7] Hossain MM. Therapeutic orchids: traditional uses and recent advances - an overview. Fitoterapia 2011;82:102–40. https://doi.org/10.1016/j.fitote.2010.09.007.
[8] Mukherjee PK, Harwansh RK, Bahadur S, Banerjee S, Kar A, Chanda J, et al. Development of Ayurveda - tradition to trend. J Ethnopharmacol 2017;197:10–24. https://doi.org/10.1016/j.jep.2016.09.024.
[9] Patwardhan B. Where lies the future of Ayurveda-inspired drug discovery? Expert Opin Drug Discov 2023;18:947–9. https://doi.org/10.1080/17460441.2023.2228201.
[10] Nedungadi P, Salethoor SN, Puthiyedath R, Nair VK, Kessler C, Raman R. Ayurveda research: emerging trends and mapping to sustainable development goals. J Ayurveda Integr Med 2023;14:100809.
[11] Chopra A, Doiphode VV. Ayurvedic medicine. Core concept, therapeutic principles, and current relevance. Med Clin North Am 2002;86:75–89. https://doi.org/10.1016/S0025-7125(03)00073-7.
[12] Govindaraj P, Nizamuddin S, Sharath A, Jyothi V, Rotti H, Raval R, et al. Genome-wide analysis correlates *Ayurveda prakriti*. Sci Rep 2015;5:15786. https://doi.org/10.1038/srep15786.
[13] Kunjumon R, Johnson AJ, Baby S. *Bacopa monnieri (Brahmi)*: phytochemistry and use in traditional Ayurvedic formulations. In: Amalraj A, Kuttappan S, Varma K, editors. Chemistry, biological activities and therapeutic applications of medicinal plants in Ayurveda. London: Royal Society of Chemistry; 2022. p. 176–200. https://doi.org/10.1039/9781839166211-00176.
[14] Dubey T, Chinnathambi S. Brahmi (*Bacopa monnieri*): an Ayurvedic herb against the Alzheimer's disease. Arch Biochem Biophys 2019;676:108153. https://doi.org/10.1016/j.abb.2019.108153.
[15] Jaiswal YS, Williams LL. A glimpse of Ayurveda - the forgotten history and principles of Indian traditional medicine. J Tradit Complement Med 2017;7:50–3. https://doi.org/10.1016/j.jtcme.2016.02.002.
[16] Mishra DN. Medicinal plants for the treatment of fever (*Jvaracikitsâ*) in the *Mâdhavacikitsà* tradition of India. Indian J Tradit Knowl 2009;8:352–61.
[17] Akhila VG. Management of *Sannipata Jwara* w.s.r to COVID-19 - case report. J Ayurveda Integr Med 2022;13:100416. https://doi.org/10.1016/j.jaim.2021.02.007.
[18] Houston DMJ, Bugert JJ, Denyer SP, Heard CM. Potentiated virucidal activity of pomegranate rind extract (PRE) and punicalagin against Herpes Simplex Virus (HSV) when co-administered with zinc (II) ions, and antiviral activity of PRE against HSV and aciclovir-resistant HSV. PLoS One 2017;12:e0179291. https://doi.org/10.1371/journal.pone.0179291.
[19] Acquadro S, Civra A, Cagliero C, Marengo A, Rittà M, Francese R, et al. *Punica granatum* leaf ethanolic extract and ellagic acid as inhibitors of Zika virus infection. Planta Med 2020;86:1363–74. https://doi.org/10.1055/a-1232-5705.
[20] Rehman S, Ashfaq UA, Ijaz B, Riazuddin S. Anti-hepatitis C virus activity and synergistic effect of *Nymphaea alba* extracts and bioactive constituents in liver infected cells. Microb Pathog 2018;121:198–209. https://doi.org/10.1016/j.micpath.2018.05.023.
[21] Almeida KB, Araujo JL, Cavalcanti JF, Romanos MTV, Mourão SC, Amaral ACF, et al. *In vitro* release and anti-herpetic activity of *Cymbopogon citratus* volatile oil-loaded nanogel. Rev Bras Farmacogn 2018;28:495–502. https://doi.org/10.1016/j.bjp.2018.05.007.
[22] Yao X, Ling Y, Guo S, Wu W, He S, Zhang Q, et al. Tatanan A from the *Acorus calamus* L. root inhibited dengue virus proliferation and infections.

Phytomedicine 2018;42:258–67. https://doi.org/10.1016/j.phymed.2018.03.018.
[23] Ye Y, Li B. 1′S-1′-Acetoxychavicol acetate isolated from *Alpinia galanga* inhibits human immunodeficiency virus type 1 replication by blocking Rev transport. J Gen Virol 2006;87:2047–53. https://doi.org/10.1099/vir.0.81685-0.
[24] Wiart C, Kumar K, Yusof MY, Hamimah H, Fauzi ZM, Sulaiman M. Antiviral properties of ent-labdene diterpenes of *Andrographis paniculata* Nees, inhibitors of herpes simplex virus type 1. Phytother Res 2005;19:1069–70. https://doi.org/10.1002/ptr.1765.
[25] Sa-Ngiamsuntorn K, Suksatu A, Pewkliang Y, Thongsri P, Kanjanasirirat P, Manopwisedjaroen S, et al. Anti-SARS-CoV-2 activity of *Andrographis paniculata* extract and its major component andrographolide in human lung epithelial cells and cytotoxicity evaluation in major organ cell representatives. J Nat Prod 2021;84:1261–70. https://doi.org/10.1021/acs.jnatprod.0c01324.
[26] Wang CH, Li W, Qiu RX, Jiang MM, Li GQ. A new diterpenoid from the aerial parts of *Andrographis paniculata*. Nat Prod Commun 2014;9:13–4. https://doi.org/10.1177/1934578x1400900105.
[27] Chen JL, Blanc P, Stoddart CA, Bogan M, Rozhon EJ, Parkinson N, et al. New iridoids from the medicinal plant *Barleria prionitis* with potent activity against respiratory syncytial virus. J Nat Prod 1998;61:1295–7. https://doi.org/10.1021/np980086y.
[28] von Rhein C, Weidner T, Henß L, Martin J, Weber C, Sliva K, et al. Curcumin and *Boswellia serrata* gum resin extract inhibit Chikungunya and Vesicular Stomatitis Virus infections *in vitro*. Antiviral Res 2016;125:51–7. https://doi.org/10.1016/j.antiviral.2015.11.007.
[29] Zhang X, He J, Huang W, Huang H, Zhang Z, Wang J, et al. Antiviral activity of the sesquiterpene lactones from *Centipeda minima* against influenza a virus *in vitro*. Nat Prod Commun 2018;13:115–9. https://doi.org/10.1177/1934578x1801300201.
[30] Zhang X, Xia Y, Yang L, He J, Li Y, Xia C, Brevilin A. A sesquiterpene lactone, inhibits the replication of influenza a virus *in vitro* and *in vivo*. Viruses 2019;11:835. https://doi.org/10.3390/v11090835.
[31] Dao TT, Nguyen PH, Won HK, Kim EH, Park J, Won BY, et al. Curcuminoids from *Curcuma longa* and their inhibitory activities on influenza A neuraminidases. Food Chem 2012;134:21–8. https://doi.org/10.1016/j.foodchem.2012.02.015.
[32] Zandi K, Ramedani E, Mohammadi K, Tajbakhsh S, Deilami I, Rastian Z, et al. Evaluation of antiviral activities of curcumin derivatives against HSV-1 in Vero cell line. Nat Prod Commun 2010;5:1935–8.
[33] Ti H, Mai Z, Wang Z, Zhang W, Xiao M, Yang Z, et al. Bisabolane-type sesquiterpenoids from: *Curcuma longa* L. exert anti-influenza and anti-inflammatory activities through NF-κB/MAPK and RIG-1/STAT1/2 signaling pathways. Food Funct 2021;12:6697–711. https://doi.org/10.1039/d1fo01212f.
[34] Krishnan K, Khanna VG, Hameed S. Antiviral activity of dasyscyphin C extracted from *Eclipta prostrata* against fish nodavirus. J Antivirals Antiretrovir 2010;2:29–32. https://doi.org/10.4172/jaa.1000018.
[35] Corona A, Seibt S, Schaller D, Schobert R, Volkamer A, Biersack B, et al. Garcinol from *Garcinia indica* inhibits HIV-1 reverse transcriptase-associated ribonuclease H. Arch Pharm (Weinheim) 2021;354:e2100123. https://doi.org/10.1002/ardp.202100123.
[36] Ashfaq UA, Masoud MS, Nawaz Z, Riazuddin S. Glycyrrhizin as antiviral agent against hepatitis C virus. J Transl Med 2011;9:1–7. https://doi.org/10.1186/1479-5876-9-112.
[37] Esposito F, Mandrone M, Del Vecchio C, Carli I, Distinto S, Corona A, et al. Multi-target activity of *Hemidesmus indicus* decoction against innovative HIV-1 drug targets and characterization of lupeol mode of action. Pathog Dis 2017;75:1–5. https://doi.org/10.1093/femspd/ftx065.
[38] Zhao G, Yin Z, Dong J. Antiviral efficacy against hepatitis B virus replication of oleuropein isolated from *Jasminum officinale* L. var. *grandiflorum*. J Ethnopharmacol 2009;125:265–8. https://doi.org/10.1016/j.jep.2009.06.030.
[39] Zhao G, Yin Z, Liu L, Mao X, Su Z. Anti-hepatitis B virus activity of 8-epi-kingiside in *Jasminum officinale* var. *grandiflorum*. Chinese Herb Med 2013;5:53–7. https://doi.org/10.7501/j.issn.1674-6384.2013.01.006.
[40] Pang X, Kang L-P, Fang X-M, Yu H-S, Han L-F, Zhao Y, et al. C21 steroid derivatives from the Dai herbal medicine Dai-Bai-Jie, the dried roots of *Marsdenia tenacissima*, and their screening for anti-HIV activity. J Nat Med 2018;72:166–80. https://doi.org/10.1007/s11418-017-1126-1.
[41] Kashiwada Y, Aoshima A, Ikeshiro Y, Chen Y-P, Furukawa H, Itoigawa M, et al. Anti-HIV benzylisoquinoline alkaloids and flavonoids from the leaves of *Nelumbo nucifera*, and structure-activity correlations with related alkaloids. Bioorganic Med Chem 2005;13:443–8. https://doi.org/10.1016/j.bmc.2004.10.020.
[42] Chiang LC, Ng LT, Cheng PW, Chiang W, Lin CC. Antiviral activities of extracts and selected pure constituents of *Ocimum basilicum*. Clin Exp Pharmacol Physiol 2005;32:811–6. https://doi.org/10.1111/j.1440-1681.2005.04270.x.
[43] Liu Q, Wang Y-F, Chen R-J, Zhang M-Y, Wang Y-F, Yang C-R, et al. Anti-coxsackie virus B3 norsesquiterpenoids from the roots of *Phyllanthus emblica*. J Nat Prod 2009;72:969–72. https://doi.org/10.1021/np800792d.
[44] Liu S, Wei W, Shi K, Cao X, Zhou M, Liu Z. *In vitro* and *in vivo* anti-hepatitis B virus activities of the lignan niranthin isolated from *Phyllanthus niruri* L. J Ethnopharmacol 2014;155:1061–7. https://doi.org/10.1016/j.jep.2014.05.064.
[45] Liu S, Wei W, Li Y, Lin X, Shi K, Cao X, et al. *In vitro* and *in vivo* anti-hepatitis B virus activities of the lignan nirtetralin B isolated from *Phyllanthus niruri* L. J Ethnopharmacol 2014;157:62–8. https://doi.org/10.1016/j.jep.2014.09.019.
[46] Arunkumar J, Rajarajan S. Study on antiviral activities, drug-likeness and molecular docking of bioactive compounds of *Punica granatum* L. to Herpes simplex virus-2 (HSV-2). Microb Pathog 2018;118:301–9. https://doi.org/10.1016/j.micpath.2018.03.052.
[47] Angamuthu D, Purushothaman I, Kothandan S, Swaminathan R. Antiviral study on *Punica granatum* L., *Momordica charantia* L., *Andrographis paniculata* Nees, and *Melia azedarach* L. to human herpes virus-3. Eur J Integr Med 2019;28:98–108. https://doi.org/10.1016/j.eujim.2019.04.008.
[48] Sanna C, Marengo A, Acquadro S, Caredda A, Lai R, Corona A, et al. *In vitro* anti-HIV-1 reverse transcriptase and integrase properties of *Punica granatum* L. leaves, bark, and peel extracts and their main compounds. Plants 2021;10:2124. https://doi.org/10.3390/plants10102124.
[49] Ho LK, Don MJ, Chen HC, Yeh SF, Chen JM. Inhibition of hepatitis B surface antigen secretion on human hepatoma cells. Components from *Rubia cordifolia*. J Nat Prod 1996;59:330–3. https://doi.org/10.1021/np960200h.
[50] Woo SY, Win NN, Noe Oo WM, Ngwe H, Ito T, Abe I, et al. Viral protein R inhibitors from *Swertia chirata* of Myanmar. J Biosci Bioeng 2019;128:445–9. https://doi.org/10.1016/j.jbiosc.2019.04.006.
[51] Kesharwani A, Polachira SK, Nair R, Agarwal A, Mishra NN, Gupta SK. Anti-HSV-2 activity of *Terminalia chebula* Retz extract and its constituents, chebulagic and chebulinic acids. BMC Complement Altern Med 2017;17:110. https://doi.org/10.1186/s12906-017-1620-8.
[52] Ajala OS, Jukov A, Ma C-M. Hepatitis C virus inhibitory hydrolysable tannins from the fruits of *Terminalia chebula*. Fitoterapia 2014;99:117–23. https://doi.org/10.1016/j.fitote.2014.09.014.
[53] Ahn M-J, Chul YK, Ji SL, Kim TG, Kim SH, Lee C-K, et al. Inhibition of HIV-1 integrase by galloyl glucoses from *Terminalia chebula* and flavonol glycoside gallates from *Euphorbia pekinensis*. Planta Med 2002;68:457–9. https://doi.org/10.1055/s-2002-32070.
[54] Denyer CV, Jackson P, Loakes DM, Ellis MR, Young DAB. Isolation of antirhinoviral sesquiterpenes from ginger (*Zingiber officinale*). J Nat Prod 1994;57:658–62. https://doi.org/10.1021/np50107a017.
[55] Hong E-H, Song JH, Kang KB, Sung SH, Ko H-J, Yang H, et al. Anti-influenza activity of betulinic acid from *Zizyphus Jujuba* on influenza A/PR/8 virus. Biomol Ther (Seoul) 2015;23:345–9. https://doi.org/10.4062/biomolther.2015.019.
[56] Kang KB, Ming G, Kim GJ, Ha TKQ, Choi H, Oh WK, et al. Jubanines F-J, cyclopeptide alkaloids from the roots of *Ziziphus jujuba*. Phytochemistry 2015;119:90–5. https://doi.org/10.1016/j.phytochem.2015.09.001.
[57] Utomo RY, Ikawati M, Meiyanto E. Revealing the potency of citrus and galangal constituents to halt SARS-CoV-2 infection. Preprints 2020;2020:2020030214. https://doi.org/10.20944/preprints202003.0214.v1.
[58] Ram TS, Munikumar M, Raju VN, Devaraj P, Boiroju NK, Hemalatha R, et al. *In silico* evaluation of the compounds of the ayurvedic drug, AYUSH-64, for the action against the SARS-CoV-2 main protease. J Ayurveda Integr Med 2022;13:100413. https://doi.org/10.1016/j.jaim.2021.02.004.
[59] Murugan NA, Pandian CJ, Jeyakanthan J. Computational investigation on *Andrographis paniculata* phytochemicals to evaluate their potency against SARS-CoV-2 in comparison to known antiviral compounds in drug trials. J Biomol Struct Dyn 2021;39:4415–26. https://doi.org/10.1080/07391102.2020.1777901.
[60] Kaushik S, Dar L, Kaushik S, Yadav JP. Identification and characterization of new potent inhibitors of dengue virus NS5 proteinase from *Andrographis paniculata* supercritical extracts on in animal cell culture and *in silico* approaches. J Ethnopharmacol 2021;267:113541. https://doi.org/10.1016/j.jep.2020.113541.
[61] Thirumoorthy G, Tarachand SP, Nagella P, Lakshmaiah VV. Identification of potential ZIKV NS2B-NS3 protease inhibitors from *Andrographis paniculata*: an *in silico* approach. J Biomol Struct Dyn 2022;40:11203–5. https://doi.org/10.1080/07391102.2021.1956592.
[62] Seniya C, Shrivastava S, Singh SK, Khan GJ. Analyzing the interaction of a herbal compound andrographolide from *Andrographis paniculata* as a folklore against swine flu (H1N1). Asian Pacific J Trop Dis 2014;4:S624–30. https://doi.org/10.1016/S2222-1808(14)60692-7.
[63] Chikhale RV, Sinha SK, Patil RB, Wabaidur SM, Patil SA, Islam MA. *In-silico* investigation of phytochemicals from *Asparagus racemosus* as plausible antiviral agent in COVID-19. J Biomol Struct Dyn 2021;39:5033–47. https://doi.org/10.1080/07391102.2020.1784289.
[64] Ashfaq UA, Jalil A, Ul Qamar MT. Antiviral phytochemicals identification from *Azadirachta indica* leaves against HCV NS3 protease: an *in silico* approach. Nat Prod Res 2016;30:1866–9. https://doi.org/10.1080/14786419.2015.1075527.
[65] Rutwick Surya U, Praveen N. A molecular docking study of SARS-CoV-2 main protease against phytochemicals of *Boerhavia diffusa* Linn. for novel COVID-19 drug discovery. Virusdisease 2021;32:46–54. https://doi.org/10.1007/s13337-021-00683-6.
[66] Roy A, Menon T. Evaluation of bioactive compounds from *Boswellia serrata* against SARS-CoV-2. Vegetos 2022;35:404–14. https://doi.org/10.1007/s42535-021-00318-7.
[67] Haridas M, Sasidhar V, Nath P, Abhithaj J, Sabu A, Rammanohar P. Compounds of *Citrus medica* and *Zingiber officinale* for COVID-19 inhibition: *in silico* evidence for cues from Ayurveda. Futur J Pharm Sci 2021;7:13. https://doi.org/10.1186/s43094-020-00171-6.
[68] Elsbaey M, Ibrahim MAA, Bar FA, Elgazar AA. Chemical constituents from coconut waste and their *in silico* evaluation as potential antiviral agents against SARS-CoV-2. South African J Bot 2021;141:278–89. https://doi.org/10.1016/j.sajb.2021.05.018.
[69] Kumar SB, Krishna S, Pradeep S, Mathews DE, Pattabiraman R, Murahari M, et al. Screening of natural compounds from *Cyperus rotundus* Linn against SARS-CoV-2

main protease (Mpro): an integrated computational approach. Comput Biol Med 2021;134:104524. https://doi.org/10.1016/j.compbiomed.2021.104524.
[70] Srivastava V, Yadav A, Sarkar P. Molecular docking and ADMET study of bioactive compounds of *Glycyrrhiza glabra* against main protease of SARS-CoV2. Mater Today Proc 2020;49:2999–3007. https://doi.org/10.1016/j.matpr.2020.10.055.
[71] Bag A, Bag A. Treatment of COVID-19 patients: *Justicia adhatoda* leaves extract is a strong remedy for COVID-19 - case report analysis and docking based study. Biol Med Chem 2020:1–7.
[72] Ghosh R, Chakraborty A, Biswas A, Chowdhuri S. Identification of alkaloids from *Justicia adhatoda* as potent SARS CoV-2 main protease inhibitors: an *in silico* perspective. J Mol Struct 2021;229:129489. https://doi.org/10.1016/j.molstruc.2020.129489.
[73] Kumar BS, Anuragh S, Kammala AK, Ilango K. Computer aided drug design approach to screen phytoconstituents of *Adhatoda vasica* as potential inhibitors of SARS-CoV-2 main protease enzyme. Life 2022;12:315. https://doi.org/10.3390/life12020315.
[74] Liao T, Cao J, Yang Z, Cheng J, Lu J. Leaf and flower extracts of six Michelia L.: polyphenolic composition, antioxidant, antibacterial activities and in vitro inhibition of α-amylase and α-glucosidase. Chem Biodivers 2022;19:e202100894. https://doi.org/10.1002/cbdv.202100894.
[75] Gopal SK, Rangasamy M, Balasubramaniam N. *In-silico* docking analysis of phytochemicals from *Mimosa pudica* L. leaves as an antiviral agent against herpes simplex virus type I. Int J Biomed Nanoletters 2021;1:1–9.
[76] Sakshi C, Harikrishnan A, Jayaraman S, Choudhury AR, Veena V. Predictive medicinal metabolites from *Momordica dioica* against comorbidity related proteins of SARS-CoV-2 infections. J Biomol Struct Dyn 2022;40:5175–88. https://doi.org/10.1080/07391102.2020.1868340.
[77] Shah S, Chaple D, Arora S, Yende S, Moharir K, Lohiya G. Exploring the active constituents of *Oroxylum indicum* in intervention of novel coronavirus (COVID-19) based on molecular docking method. Netw Model Anal Health Inform Bioinform 2021;10:1–12. https://doi.org/10.1007/s13721-020-00279-y.
[78] Lakhera S, Devlal K, Ghosh A, Rana M. *In silico* investigation of phytoconstituents of medicinal herb '*Piper longum*' against SARS-CoV-2 by molecular docking and molecular dynamics analysis. Results Chem 2021;3:100199. https://doi.org/10.1016/j.rechem.2021.100199.
[79] Lakhera S, Devlal K, Ghosh A, Rana M. In silico investigation of phytoconstituents of medicinal herb 'Piper Longum' against SARS- CoV-2 by molecular docking and molecular dynamics analysis. Results Chem 2021;3:100199. https://doi.org/10.1016/j.rechem.2021.100199.
[80] Choudhary P, Chakdar H, Singh D, Selvaraj C, Singh SK, Kumar S, et al. Computational studies reveal piperine, the predominant oleoresin of black pepper (*Piper nigrum*) as a potential inhibitor of SARS-CoV-2 (COVID-19). Curr Sci 2020;119:1333–42. https://doi.org/10.18520/cs/v119/i8/1333-1342.
[81] Patil VS, Harish DR, Vetrivel U, Roy S, Deshpande SH, Hegde HV, et al. Hepatitis C Virus NS3/4A Inhibition and host immunomodulation by tannins from *Terminalia chebula*: a structural perspective. Molecules 2022;27:1076. https://doi.org/10.3390/molecules27031076.
[82] Gupta PP, Nayak SU, Parab MM, Dasgupta D, Harit MS. Computational modeling and analysis of Ayurvedic compounds in fighting against COVID-19. J Drug Res Ayurvedic Sci 2021;6:28–39. https://doi.org/10.4103/jdras.jdras_11_21.
[83] Jannat K, Hasan A, Al Mahamud R, Jahan R, Bondhon TA, Farzana B-n, et al. *In silico* screening of *Vigna radiata* and *Vigna mungo* phytochemicals for their binding affinity to SARS-CoV-2 (COVID-19) main protease (3CL pro). J Med Plants Stud 2020;8:89–95.
[84] Srivastava A, Siddiqui S, Ahmad R, Mehrotra S, Ahmad B, Srivastava AN, et al. Exploring nature's bounty: identification of *Withania somnifera* as a promising source of therapeutic agents against COVID-19 by virtual screening and *in silico* evaluation. J Biomol Struct Dyn 2022;40:1858–908. https://doi.org/10.1080/07391102.2020.1835725.
[85] Pandey P, Singhal D, Khan F, Arif M. An *in silico* screening on *Piper nigrum, Syzygium aromaticum* and *Zingiber officinale* roscoe derived compounds against SARSCOV2: a drug repurposing approach. Biointerface Res Appl Chem 2021;11:11122–34. https://doi.org/10.33263/BRIAC114.1112211134.
[86] Zubair MS, Maulana S, Widodo A, Pitopang R, Arba M, Hariono M, et al. GC-MS, LC-MS/MS, docking and molecular dynamics approaches to identify potential SARS-COV-2 3-chymotrypsin-like protease inhibitors from *Zingiber officinale* Roscoe. Molecules 2021;26:5230. https://doi.org/10.3390/molecules26175230.
[87] Shakiba Y, Rezatofighi SE, Nejad SMS, Ardakani MR. Antiviral activity of *Alhagi maurorum* Medik's methanolic extract on foot and mouth disease virus (FMDV) in cell cultures. Jundishapur J Nat Pharm Prod 2016;11:4–8. https://doi.org/10.17795/jjnpp-30641.
[88] Ling APK, Khoo BF, Seah CH, Foo KY, Cheah RK, Chye SM, et al. Inhibitory activities of methanol extracts of *Andrographis paniculata* and *Ocimum sanctum* against Dengue-1 virus. International Conference on Biological, Environment and Food Engineering (BEFE-2014), August 4-5, 2014 Bali (Indonesia) 2014:47–52. https://doi.org/10.15242/iicbe.c814013.
[89] Yeh CF, Chang JS, Wang KC, Shieh DE, Chiang LC. Water extract of *Cinnamomum cassia* Blume inhibited human respiratory syncytial virus by preventing viral attachment, internalization, and syncytium formation. J Ethnopharmacol 2013;147:321–6. https://doi.org/10.1016/j.jep.2013.03.010.
[90] Sood R, Raut R, Tyagi P, Pareek PK, Barman TK, Singhal S, et al. *Cissampelos pareira* Linn: natural source of potent antiviral activity against all four Dengue virus serotypes. PLoS Negl Trop Dis 2015;9:1–20. https://doi.org/10.1371/journal.pntd.0004255.
[91] Haider M, Dholakia D, Panwar A, Garg P, Anand V, Gheware A, et al. Traditional use of *Cissampelos pareira* L. for hormone disorder and fever provides molecular links of ESR1 modulation to viral inhibition. bioRxiv 2021:2021. https://doi.org/10.1101/2021.02.17.431579.
[92] Esquenazi D, Wigg MD, Miranda MMFS, Rodrigues HM, Tostes JBF, Rozental S, et al. Antimicrobial and antiviral activities of polyphenolics from *Cocos nucifera* Linn. (Palmae) husk fiber extract. Res Microbiol 2002;153:647–52. https://doi.org/10.1016/S0923-2508(02)01377-3.
[93] Ichsyani M, Ridhanya A, Risanti M, Desti H, Ceria R, Putri DH, et al. Antiviral effects of *Curcuma longa* L. against dengue virus *in vitro* and *in vivo*. IOP Conf Ser Earth Environ Sci 2017;101. https://doi.org/10.1088/1755-1315/101/1/012005.
[94] Wahyuni TS, Permatasari AA, Widiandani T, Fuad A, Widyawaruyanti A, Aoki-Utsubo C, et al. Antiviral activities of *Curcuma* genus against hepatitis C virus. Nat Prod Commun 2018;13:1579–82. https://doi.org/10.1177/1934578x1801301204.
[95] Jyotirmayee B, Mahalik G. A review on selected pharmacological activities of Curcuma longa L. Int J Food Prop 2022;25:1377–98. https://doi.org/10.1080/10942912.2022.2082464.
[96] Kuo YC, Lin YL, Liu CP, Tsai WJ. Herpes simplex virus type 1 propagation in HeLa cells interrupted by *Nelumbo nucifera*. J Biomed Sci 2005;12:1021–34. https://doi.org/10.1007/s11373-005-9001-6.
[97] Wahyuni TS, Azmi D, Permanasari AA, Adianti M, Lydia T, Widiandani T, et al. Anti-viral activity of *Phyllanthus niruri* against hepatitis C virus. Malays Appl Biol 2019;48:105–11.
[98] Moradi MT, Karimi A, Shahrani M, Hashemi L, Ghaffari-Goosheh MS. Anti-influenza virus activity and phenolic content of pomegranate (*Punica granatum* L.) peel extract and fractions. Avicenna J Med Biotechnol (AJMB) 2019;11:285–91.
[99] Salles TS, Meneses MDF, Caldas LA, Sá-Guimarães TE, de Oliveira DM, Ventura JA, et al. Virucidal and antiviral activities of pomegranate (*Punica granatum*) extract against the mosquito-borne Mayaro virus. Parasites Vectors 2021;14:443. https://doi.org/10.1186/s13071-021-04955-4.
[100] Caruso A, Barbarossa A, Tassone A, Ceramella J, Carocci A, Catalano A, et al. Pomegranate: Nutraceutical with promising benefits on human health. Appl Sci 2020;10:6915. https://doi.org/10.3390/app10196915.
[101] Salles TS, Meneses MDF, Caldas LA, Sá-Guimarães TE, de Oliveira DM, Ventura JA, et al. Virucidal and antiviral activity of extract of *Punica granatum* cultivated in Brazil. Parasites Vectors 2021:1–12. https://doi.org/10.21203/rs.3.rs-214931/v1.
[102] Arthanari S, Renukadevi P, Vanitha J, Venkateshwaran K, Ganesh M, De Clercq E. Evaluation of antiviral and cytotoxic activities of methanolic extract of *Thespesia populnea* (Malvaceae) flowers. J Herbs, Spices, Med Plants 2011;17:386–91. https://doi.org/10.1080/10496475.2011.605514.
[103] Zannella C, Giugliano R, Chianese A, Buonocore C, Vitale GA, Sanna G, et al. Antiviral activity of *Vitis vinifera* leaf extract against SARS-COV-2 and HSV-1. Viruses 2021;13:1263. https://doi.org/10.3390/v13071263.
[104] Agostinho KF, Rechenchoski DZ, Faccin-Galhardi LC, de Sousa ALN, Cunha AP, Ricardo NMPS, et al. *Cucumis melo* pectin as potential candidate to control herpes simplex virus infection. FEMS Microbiol Lett 2021;368:2014–8. https://doi.org/10.1093/femsle/fnab013.
[105] Kurskaya O, Prokopyeva E, Bi H, Sobolev I, Murashkina T, Shestopalov A, et al. Anti-influenza activity of medicinal material extracts from Qinghai-Tibet Plateau. Viruses 2022;14:1–10. https://doi.org/10.3390/v14020360.
[106] Jiang Y, Ng TB, Liu Z, Wang C, Li N, Qioa W, et al. Immunoregulatory and anti-HIV-1 enzyme activities of antioxidant components from lotus (*Nelumbo nucifera* Gaertn.) rhizome. Biosci Rep 2011;31:381–90. https://doi.org/10.1042/BSR20100062.
[107] Taghizadeh SF, Azizi M, Asili J, Madarshahi FS, Rakhshandeh H, Fujii Y. Therapeutic peptides of *Mucuna pruriens* L.: anti-genotoxic molecules against human hepatocellular carcinoma and hepatitis C virus. Food Sci Nutr 2021;9:2908–14. https://doi.org/10.1002/fsn3.2248.
[108] Dhama K, Sharun K, Gugjoo MB, Tiwari R, Alagawany M, Yatoo MI, et al. A comprehensive review on chemical profile and pharmacological activities of Ocimum basilicum. Food Rev Int 2023;39:119–47. https://doi.org/10.1080/87559129.2021.1900230.
[109] Silprasit K, Seetaha S, Pongsanaraku P, Hannongbua S, Choowongkomon K. Anti-HIV-1 reverse transcriptase activities of hexane extracts from some Asian medicinal plants. J Med Plant Res 2011;5:4899–906.
[110] Xu J, Song X, Yin ZQ, Cheng AC, Jia RY, Deng YX, et al. Antiviral activity and mode of action of extracts from neem seed kernel against duck plague virus *in vitro*. Poult Sci 2012;91:2802–7. https://doi.org/10.3382/ps.2012-02468.
[111] Melk MM, El-Hawary SS, Melek FR, Saleh DO, Ali OM, El Raey MA, et al. Antiviral activity of zinc oxide nanoparticles mediated by *Plumbago indica* L. extract against Herpes Simplex Virus Type 1 (HSV-1). Int J Nanomedicine 2021;16:8221–33. https://doi.org/10.2147/IJN.S339404.
[112] Modi M, Nutan Pancholi B, Kulshrestha S, Rawat AJ, Malhotra S, et al. Anti-HIV-1 activity, protease inhibition and safety profile of extracts prepared from *Rhus parviflora*. BMC Complement Altern Med 2013;13:158. https://doi.org/10.1186/1472-6882-13-158.
[113] Hashmi S, Begum W, Sultana A. Efficacy of Sphaeranthus indicus and cream of Lawsonia inermis in cervical erosion with cervicitis. Eur J Int Med 2011;3:e183–8. https://doi.org/10.1016/j.eujim.2011.08.002.
[114] Nguyen PQT, Ooi JSG, Nguyen NTK, Wang S, Huang M, Liu DX, et al. Antiviral cystine knot α-amylase inhibitors from *Alstonia scholaris*. J Biol Chem 2015;290:31138–50. https://doi.org/10.1074/jbc.M115.654855.

[115] Haider M, Anand V, Enayathullah MG, Parekh Y, Ram S, Kumari S, et al. Anti-SARS-CoV-2 potential of *Cissampelos pareira* L. identified by connectivity map-based analysis and *in vitro* studies. BMC Complement Med Ther 2022;22:114. https://doi.org/10.1186/s12906-022-03584-3.

[116] Murali KS, Sivasubramanian S, Vincent S, Murugan SB, Giridaran B, Dinesh S, et al. Anti-chikungunya activity of luteolin and apigenin rich fraction from *Cynodon dactylon*. Asian Pac J Trop Med 2015;8:352–8. https://doi.org/10.1016/S1995-7645(14)60343-6.

[117] Jha RK, Wisoyo SD, Srisombat S. Study on the efficacy of *Cynodon dactylon* against infectious myonecrosis virus (IMNV) in *Penaeus vannamei*. bioRxiv 2020; 2020. https://doi.org/10.1101/2020.11.09.374074.

[118] Beuscher N, Bodinet C, Neumann-Haefelin D, Marston A, Hostettmann K. Antiviral activity of African medicinal plants. J Ethnopharmacol 1994;42:101–9. https://doi.org/10.1016/0378-8741(94)90103-1.

[119] Roy S, Chaurvedi P, Chowdhary A. Evaluation of antiviral activity of essential oil of *Trachyspermum ammi* against Japanese encephalitis virus. Pharmacognosy Res 2015;7:263–7. https://doi.org/10.4103/0974-8490.157977.

[120] Banerjee S, Kar A, Mukherjee PK, Haldar PK, Sharma N, Katiyar CK. Immunoprotective potential of Ayurvedic herb Kalmegh (*Andrographis paniculata*) against respiratory viral infections - LC-MS/MS and network pharmacology analysis. Phytochem Anal 2021;32:629–39. https://doi.org/10.1002/pca.3011.

[121] Kowalczyk M, Golonko A, Świsłocka R, Kalinowska M, Parcheta M, Swiergiel A, et al. Drug design strategies for the treatment of viral disease. Plant phenolic compounds and their derivatives. Front Pharmacol 2021;12:709104. https://doi.org/10.3389/fphar.2021.709104.

[122] Liu R, Narita R, Nishimura H, Marumoto S, Yamamoto SP, Ouda R, et al. Antiviral activity of phenolic derivatives in pyroligneous acid from hardwood, softwood, and bamboo. ACS Sustain Chem Eng 2017;6:119–26. https://doi.org/10.1021/acssuschemeng.7b01265.

[123] Vuyolwethu K, Opeoluwa OO, Blessing AA. Antiviral activities of oleanolic acid and its analogues. Molecules 2018;23:2300. https://doi.org/10.3390/molecules23092300.

[124] Ianevski A, Yao R, Simonsen RM, Myhre V, Ravlo E, Kaynova GD, et al. Mono- and combinational drug therapies for global viral pandemic preparedness. iScience 2022;25:104112. https://doi.org/10.1016/j.isci.2022.104112.

[125] World Health Organization. Managing epidemics: key facts about major deadly diseases. Geneva: World Health Organization; 2018. p. 1–257. https://apps.who.int/iris/handle/10665/272442.

[126] Deatrick E. NIAID announces antiviral drug development awards. 2022. https://www.niaid.nih.gov/news-events/niaid-announces-antiviral-drug-development-awards. [Accessed 18 October 2024].

[127] Ali SM, Sheikh WM, Rather MA, Venkatesalu V, Bashir SM, Nabi SU. Medicinal plants: treasure for antiviral drug discovery. Phytother Res 2021;35:3447–83. https://doi.org/10.1002/ptr.7039.

[128] Sagna A, Nair RVR, Hulyalkar N, Rajasekharan S, Nair VTG, Sivakumar KC, et al. Ethyl palmitate, an anti-chikungunya virus principle from *Sauropus androgynus*, a medicinal plant used to alleviate fever in ethnomedicine. J Ethnopharmacol 2023; 309:116366. https://doi.org/10.1016/j.jep.2023.116366.

[129] Musarra-Pizzo M, Pennisi R, Ben-Amor I, Mandalari G, Sciortino MT. Antiviral activity exerted by natural products against human viruses. Viruses 2021;13:828. https://doi.org/10.3390/v13050828.